

AD-A048 168

COLORADO STATE UNIV FORT COLLINS
TROPICAL CYCLONE RESEARCH BY DATA COMPOSITING.(U)
JUL 77 W M GRAY, W M FRANK

F/G 4/2

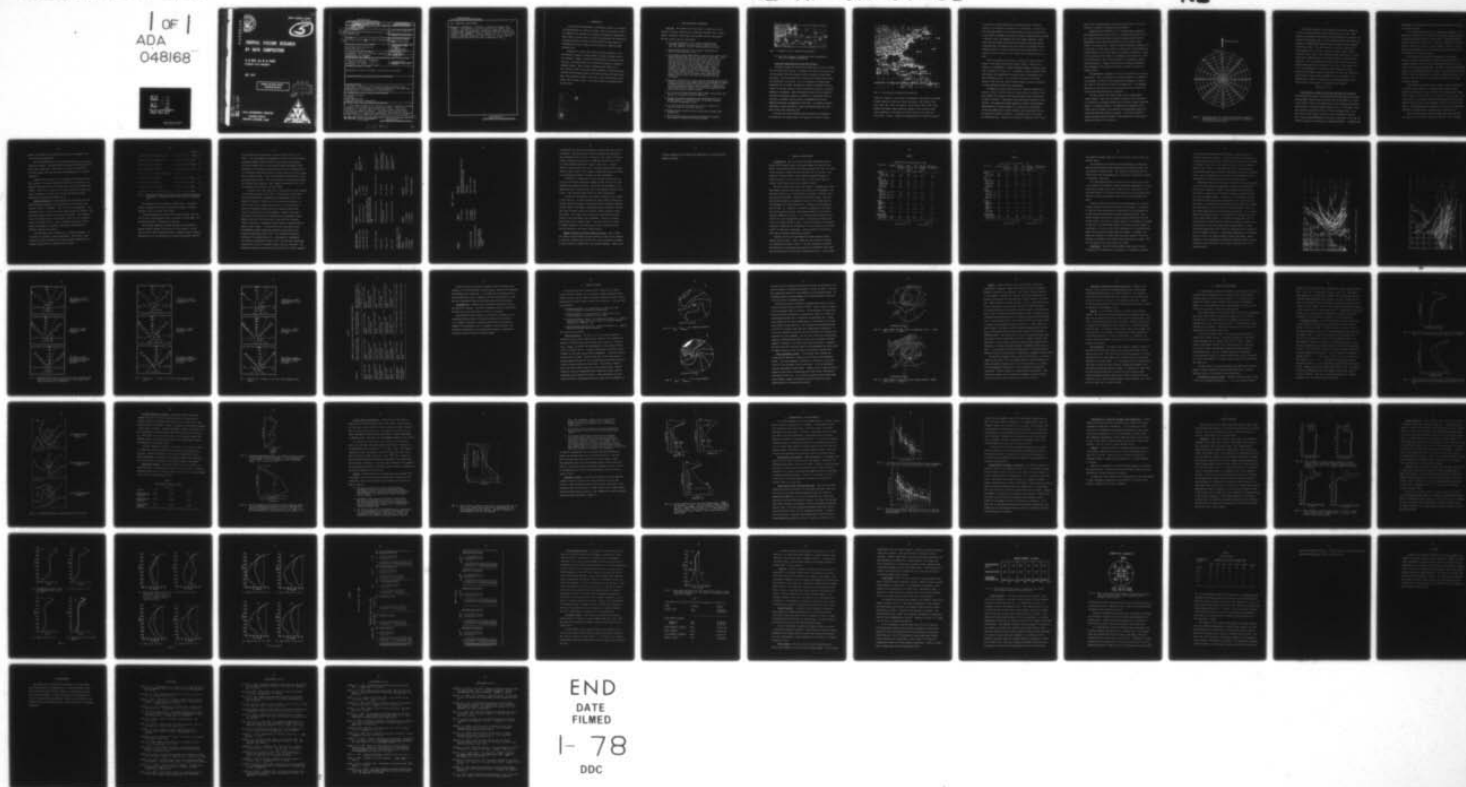
UNCLASSIFIED

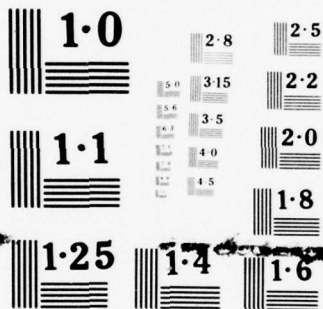
NEPRF-TR-77-01

N00228-76-C-2129

NL

1 OF 1
ADA
048168





NATIONAL BUREAU OF STANDARDS
MICROCOPY RESOLUTION TEST CHART

AD A048168



NEPRF TECHNICAL REPORT
TR - 77 - 01

5

TROPICAL CYCLONE RESEARCH BY DATA COMPOSITING

W. M. GRAY and W. M. FRANK
COLORADO STATE UNIVERSITY

JULY 1977

APPROVED FOR PUBLIC RELEASE
DISTRIBUTION UNLIMITED

DDC
RECEIVED
DEC 20 1977

AD No. _____
DDC FILE COPY

NAVAL ENVIRONMENTAL PREDICTION
RESEARCH FACILITY
MONTEREY, CALIFORNIA 93940



UNCLASSIFIED

SECURITY CLASSIFICATION OF THIS PAGE (When Data Entered)

18. REPORT DOCUMENTATION PAGE		READ INSTRUCTIONS BEFORE COMPLETING FORM	
1. REPORT NUMBER (19) NEPRE Technical Report TR-77-01	2. GOVT ACCESSION NO.	3. RECIPIENT'S CATALOG NUMBER	
4. TITLE (and Subtitle) (6) Tropical Cyclone Research By Data Compositing.		5. TYPE OF REPORT & PERIOD COVERED (9) Technical rept.	
6. PERFORMING ORG. REPORT NUMBER		7. CONTRACT OR GRANT NUMBER(s)	
7. AUTHOR(s) (10) William M./Gray and William M./Frank		(15) N00228-76-C-2129 NEW	
9. PERFORMING ORGANIZATION NAME AND ADDRESS ✓ Colorado State University Fort Collins, CO		10. PROGRAM ELEMENT, PROJECT, TASK AREA & WORK UNIT NUMBERS PN 7W0513 TA 7W0513-CC00 NEPRE WU # 6.3-2	
11. CONTROLLING OFFICE NAME AND ADDRESS Commander, Naval Air Systems Command Department of the Navy Washington, DC 20361		12. REPORT DATE (11) July 1977	
14. MONITORING AGENCY NAME & ADDRESS (if different from Controlling Office) Naval Environmental Prediction Research Facility Monterey, CA 93940 (12) 73p.		13. NUMBER OF PAGES 70	
15. SECURITY CLASS. (of this report) UNCLASSIFIED		16. DECLASSIFICATION/DOWNGRADING SCHEDULE	
16. DISTRIBUTION STATEMENT (of this Report) Approved for public release; distribution unlimited.			
17. DISTRIBUTION STATEMENT (of the abstract entered in Block 20, if different from Report)			
18. SUPPLEMENTARY NOTES Additional funding for the research reported herein was supplied by the National Science Foundation and the National Oceanographic and Atmospheric Administration.			
19. KEY WORDS (Continue on reverse side if necessary and identify by block number) Tropical Cyclones Typhoons Data Compositing Tropical Cyclone Forecasting			
20. ABSTRACT (Continue on reverse side if necessary and identify by block number) → This paper presents the results of recent tropical cyclone research at Colorado State University (CSU). Particular attention is paid to new findings which impact storm fore- casting and modeling efforts. Observational studies using large amounts of composited rawinsonde, satellite and aircraft flight data have been performed to analyze tropical cyclone			

DD FORM 1473
1 JAN 73EDITION OF 1 NOV 65 IS OBSOLETE
S N 0102-014-6601

UNCLASSIFIED

SECURITY CLASSIFICATION OF THIS PAGE (When Data Entered)

088 300

LB

UNCLASSIFIED

SECURITY CLASSIFICATION OF THIS PAGE(When Data Entered)

20. Abstract (continued)

→ dynamics, energetics, intensity, intensity change, and motion. The genesis of storms from earliest stage cloud clusters was also analyzed. Numerical modeling studies on cloud cluster dynamics and the intensification of pre-storm clusters are underway. Future research in all of the above areas is planned to exploit fully the very large tropical cyclone data set which has been assembled at CSU. ↑

UNCLASSIFIED

SECURITY CLASSIFICATION OF THIS PAGE(When Data Entered)

1. INTRODUCTION

The authors have undertaken a comprehensive study of the origins and characteristics of tropical cyclones. Many of the current results are believed to be relevant to forecasting and numerical simulations of these storms, and this report is issued to disseminate such information. The research project includes composite studies of large amounts of rawinsonde and aircraft flight data and analysis of digitized DMSP satellite data.

Chapters 3-6 of this report discuss results applicable to the forecasting of tropical cyclone movement, intensity changes, genesis and intensity. Chapter 7 presents new information concerning cyclone structure and dynamics which are of particular interest to numerical modeling studies. There are more detailed project reports (P.I. - Wm. M. Gray) on each of the above topics available or forthcoming from Colorado State University (Shea, 1972, Shea and Gray, 1973 and Gray and Shea, 1973; Ruprecht and Gray, 1976; Gray, 1975a, 1975b; George, 1975; Frank, 1976; and Zehr, 1976). Three other reports are planned within the next year.

ACCESSION No.	
NTIS	White Section <input checked="" type="checkbox"/>
GPO	Soft Section <input type="checkbox"/>
UNANNOUNCED	<input type="checkbox"/>
JUSTIFICATION.....	
BY.....	
DISTRIBUTION/AVAILABILITY CODES	
DIST.	AVAIL. and/or SPECIAL
A	

DDC
 RECEIVED
 DEC 20 1977
 RECEIVED
 D

2. DATA AND ANALYSIS TECHNIQUES

Data Set. The information in this paper is taken from various studies of tropical cyclones using composited rawinsonde data, climatological information, NOAA flight data and DMSP satellite photographs.

The data sources used are listed below:

- 1) Ten years (1961-1970) of N.W. Pacific rawinsonde data (~18,000 soundings) from 30 stations as shown in Fig. 1. This data sample is currently being expanded to 20 years.
- 2) Twenty years (1956-1975) of N. Atlantic rawinsonde data from the stations shown in Fig. 2.
- 3) All available reduced NOAA Research Flight Facility (RFF) Atlantic inner-hurricane flight data for the period of 1957-1967. This storm flight data has been described by the author and his graduate student in published papers (Shea and Gray, 1973; Gray and Shea, 1973). This aircraft data sample includes over 500 individual radial leg missions. The data itself is listed in a report by Gray and Shea (1976). This is believed to be the best available information on inner tropical storm winds, radius of maximum winds, inner radar eye radius, central pressure, etc. It is hoped that uses can be found for this in the Pacific where some degree of meshing of the aircraft data with the rawinsonde data may be possible.
- 4) Five years (1971-1975) of direct read-out from Guam Defense Meteorological Satellite Program (DMSP) satellite photographs of tropical cyclones and cloud clusters in the N.W. Pacific. This 1/3 nautical mile resolution data has been digitized and composited to perform quantitative analyses of the convection associated with West Pacific tropical weather systems.
- 5) All of the Joint Typhoon Warning Center (JTWC), Guam typhoon summaries for the 30-year period of 1946-1975.
- 6) Seasonal sea-surface temperature and thermocline data in 5° marsden squares for the whole Pacific as recently furnished by the Navy Oceanographic Office.
- 7) U.S. Navy data tape documentation of Pacific typhoons and tropical storms for the period 1946-1975.
- 8) Digitized daily satellite data for the period of October 1966 through 1970.
- 9) The new global tropical storm data tape which has recently been issued from Asheville by Harold Crutcher.

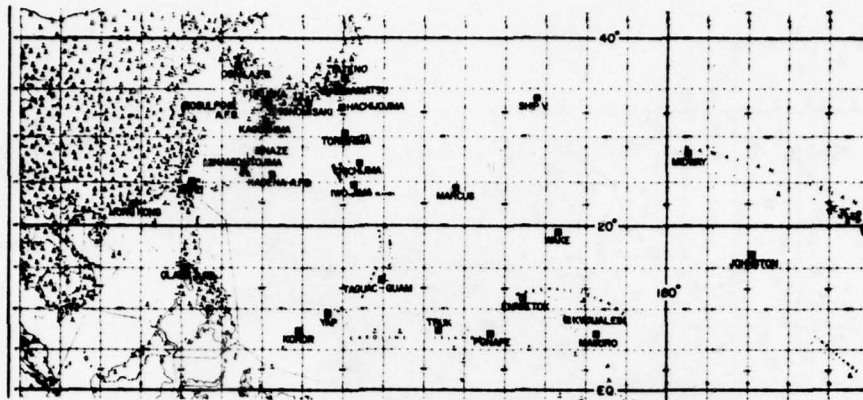


Fig. 1. Northwest Pacific rawinsonde data network.

- 10) West Indies tropical cyclone track data as supplied by Charles A. Neumann of NOAA Miami.

Rawinsonde Compositing Philosophy and Technique.

Tropical cyclones and cloud clusters spend most of their lifetimes over the warm tropical oceans. Traditional data sources are very sparse in such regions, and daily tropical weather analyses are notoriously unreliable. The severe winds found in tropical cyclones further reduce the availability of such data. It is not possible to obtain enough rawinsonde data or surface observations around any individual storm or cluster at one time period to permit quantitative analysis of structure, dynamics or energetics. High resolution satellite data are capable of achieving the necessary visual data density, but the picture data are difficult to quantify, and the number of parameters which can be measured accurately is inadequate at this time. In addition, vertical resolution is often limited by a dense cirrus shield which may cover most of the active convective area.

Aircraft data have provided the best information concerning the activities in the intense central core regions of tropical cyclones.

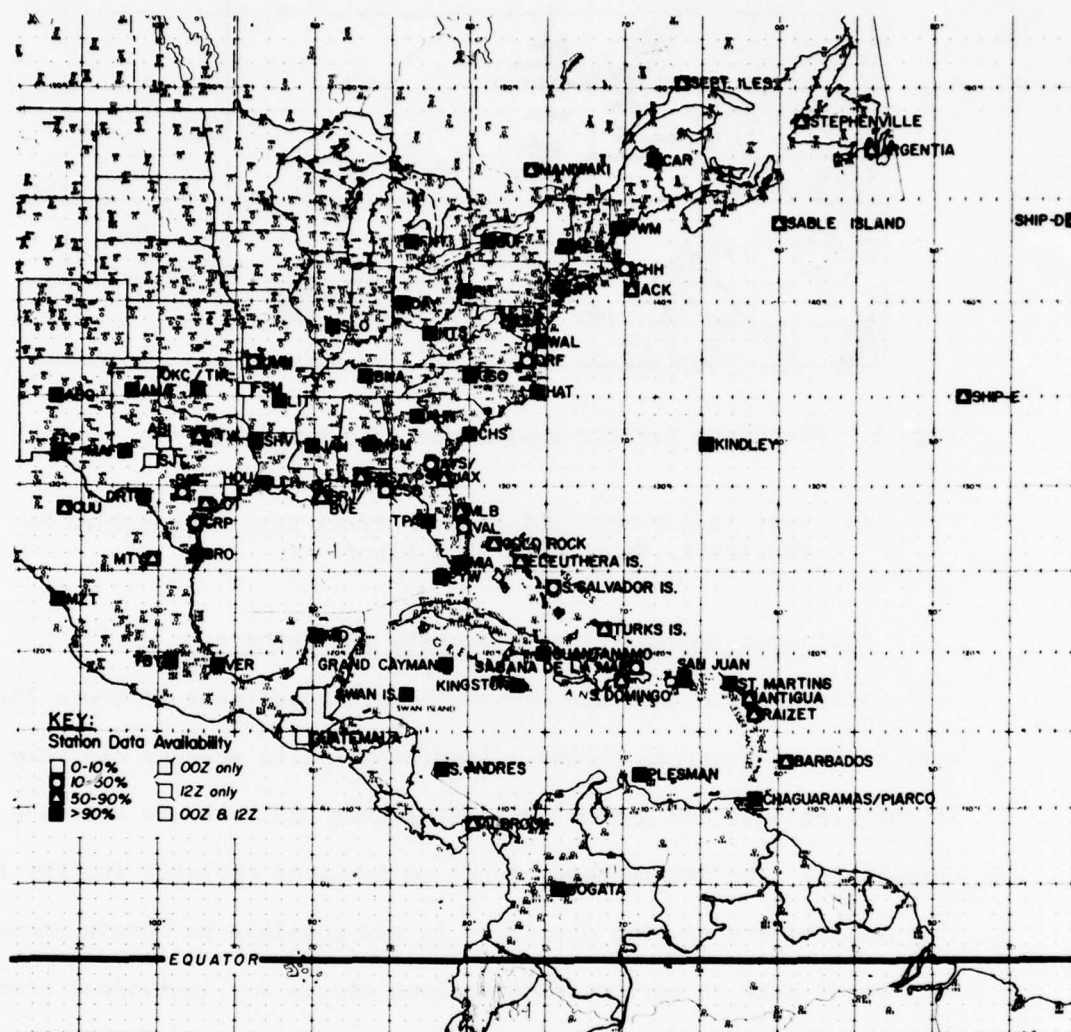


Fig. 2. North Atlantic Rawinsonde Data Network.

There are a number of case studies of individual storms based on Northwest Atlantic hurricane flight data (Riehl and Malkus, 1961; Miller, 1962; Gray, 1962, 1967; LaSeur and Hawkins, 1963; Sheets, 1967a, 1967b, 1968; Hawkins and Rubsam, 1968; Hawkins and Imbembo, 1976) and also statistical treatments of the flight data (Shea and Gray, 1973, Gray and Shea, 1973). However, logistical considerations have limited the ability

of aircraft to provide information concerning the outer convective regions of the storm and its broader scale environment. Aircraft data also have been limited to a few flight levels per storm time period due to the usually low number of available aircraft, maximum aircraft ceilings of 200 mb or less, and dangerous low level flight conditions. These latter two restrictions are particularly important since the present study shows that the maximum inflow and outflow from Northwest Pacific typhoons usually occur near cloud base and 150 mb respectively. Few aircraft studies of tropical cloud clusters were accomplished prior to GATE.

None of the above data sources can produce an accurate vertical profile of the radial wind pattern around a system. Without such a profile it is impossible to compute meaningful budgets of energy, water vapor, momentum, vorticity, etc. In addition, vertical profiles of the other dynamic and thermodynamic variables cannot be determined fully over the mesoscale area. It is necessary to composite very large amounts of data from many similar weather systems at many time periods to obtain meaningful quantitative measurements.

Although the extreme variabilities and individual asymmetries of tropical cyclones and cloud clusters are well known, the natures of the basic dynamic and energetic processes which govern these systems must be largely invariant. Compositing allows quantitative analyses of these features. Any compositing system smoothes out many of the individual characteristics of single systems, but a great deal of information concerning asymmetrical or "eddy" qualities can be deduced by the use of proper data handling techniques. The methods used in this study are discussed below. Storms are so variable at individual time periods

that to form a general physical picture of their nature, it is often desirable to smooth out individual day variability.

Compositing was performed on a 15° latitude radius cylindrical grid extending from sea level to 50 mb. The system circulation center was located at each time period using JTC reports and/or satellite photographs, and the grid was positioned with the system at grid center of the lowest level. Whenever available rawinsonde soundings fell on the grid at a given time period for a given storm, each sounding was located relative to the storm center in cylindrical coordinates. Figure 3 shows the grid and the number of soundings per grid space for a typical stratification. All of the parameters to be composited, whether directly measured or computed from the directly measured parameters, were determined at the observation station locations at 19 vertical pressure levels.

The geographical alignment of the grid varied with the coordinate system used. After all parameters were either measured or computed for each sounding, the value of each parameter was assigned to a point at the center of the grid box in which the sounding fell. All soundings which fell in that grid space for the particular group of storms and time periods being analyzed were composited.

The data set was sufficiently large to allow compositing of various subsets. Data could be grouped according to any characteristics observed in individual systems such as location, season, intensity, motion, or intensity tendency. By comparing the composites of different types of systems it was possible to quantitatively analyze the persistent differences between the groups. It was also possible to remove obviously atypical systems or time periods from a data group to improve the quality of the data set.

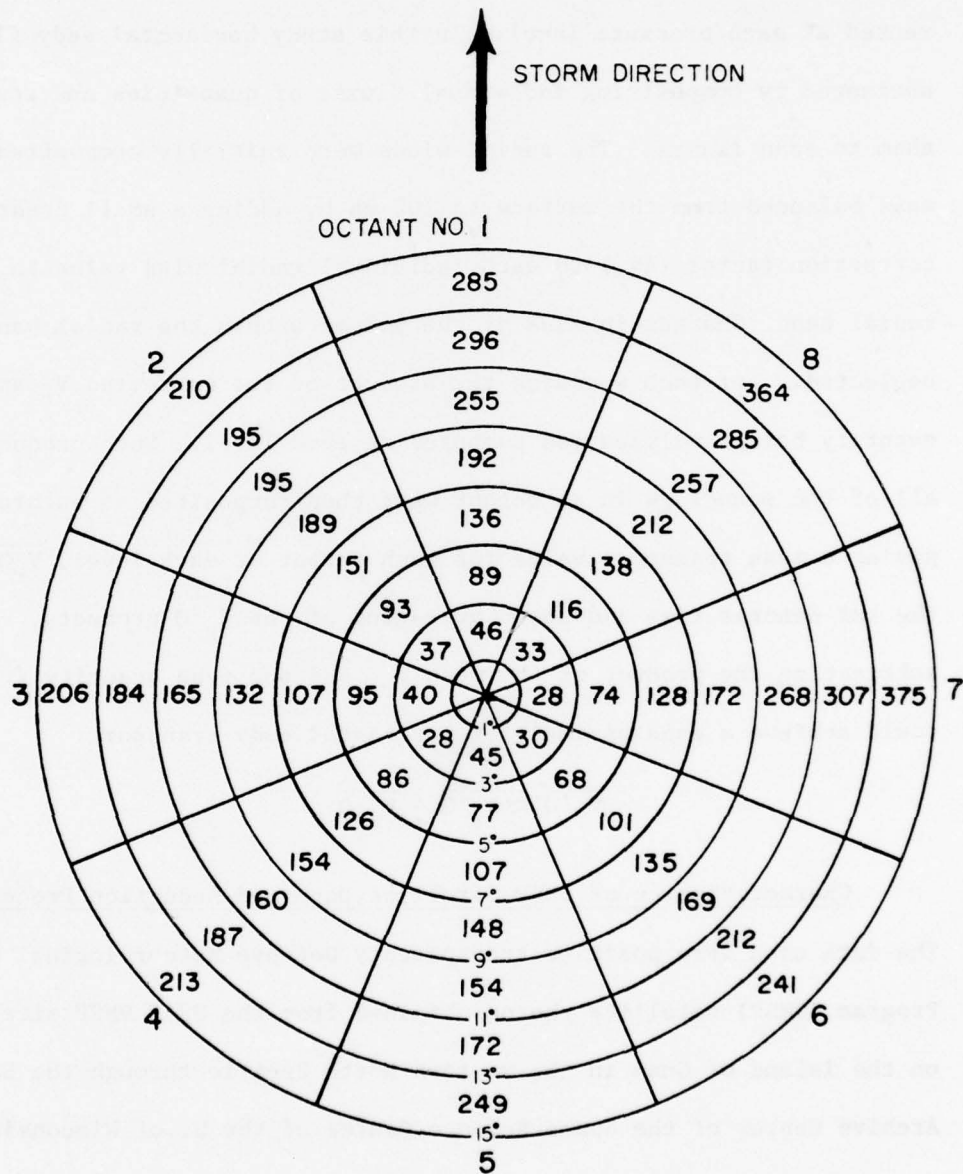


Figure 3. Compositing grid (15° latitude radius) with the number of rawinsonde reports in each octant and each 2° radial band for a typical stratification.

The relative positions of the system and the balloon changed due to their respective motions during the balloon's ascent time. These motions were estimated from the data, and the positions of each were corrected at each pressure level. In this study horizontal eddy fluxes were estimated by compositing individual fluxes of quantities and comparing them to mean fluxes. The radial winds were initially composited and mass balanced from the surface to 100 mb by adding a small constant correction factor (ΔV_r) to each individual radial wind value in a given radial band. Changes in mass of the volume within the radial band were neglected. For each sounding the product of the corrected V_r and the quantity being analyzed was computed at each level. Such products for all of the soundings in an octant were then composited as before, giving a mean transport value for each octant at each level, $\overline{V_r Q}$, where the bar denotes time and space averaging of the $V_r \cdot Q$ products. By subtracting the product of the mean $\overline{V_r}$ and the mean quantity (\overline{Q}) one could achieve a good estimate of horizontal eddy transport:

$$\overline{V_r' Q'} \approx \overline{V_r \cdot Q} - \overline{V_r} \cdot \overline{Q}$$

Characteristics of DMSP Satellite Data and Reduction Procedures.

The data used were positive transparency Defense Meteorological Satellite Program (DMSP) satellite photos obtained from the USAF DMSP site located on the island of Guam in the western North Pacific through the Satellite Archive Center of the Space Science Center of the U. of Wisconsin. This data covered the period from 1971 to 1975 and included as much of the life cycle of each tropical cyclone as could be obtained by the Guam site. This included approximately four days of data prior to the time the tropical cyclone was classified as a tropical depression. In addition 150

photographs of non-developing cloud clusters were obtained to compare to pre-storm clusters.

For a detailed satellite study of penetrative convection, it is absolutely necessary that one can count the smallest possible diameter cells which have penetrated the cirrus canopy. The DMSP VHR imagery from Guam represents a unique data set from the standpoint of overall quality, resolution (1/3 n.mi.), and the number of tropical cyclones that have been observed over a relatively long and continuous period by the same type of satellite sensor.

The Colorado State University, Department of Atmospheric Science's new Optical Data Digitizer Display (abbreviated OD³) is a specially designed research oriented system which provides the capability for digitizing transparencies. As many as 16 separate brightness levels can be distinguished with the system. The primary purpose of the OD³ is to allow the researcher to selectively prepare portions of data stored on film for further, more extensive processing in the large university computer.

Deep penetrative convection cells within a tropical disturbance or tropical cyclone display an extremely bright albedo, probably greater than 90 percent. Since this albedo far exceeds that of lower level clouds and the sea surface, it is possible to isolate these cells using the OD³. The specified density range mentioned above was determined by the OD³ as part of the brightness set-up for each new transparency. No brightness values examined on any data thus far have been found which exceeded those of the penetrative convective cells.

Only those grid squares which contained deep convective cells that were part of the storm system were digitized. Cells contained

within a grid square to be digitized that were not considered a part of the storm were blocked out.

The visual DMSP data are also being hand analyzed for penetrative convective elements. The penetrative cloud tops are outlined, and their total area is composited. This serves as a check for the OD³ since the latter system often has difficulty distinguishing all of the deep convection.

Infrared (IR) data with 2 n.mi. resolution is analyzed using the OD³ to measure the amount of high cirrus present in each system. The brightest (coldest) cirrus is stratified into three levels (temperature levels). These data are being used to study inter-storm variabilities, diurnal variations in cirrus cover and lag times between maximum penetrative convection and maximum cirrus.

Numerical Modeling. We presently have two operating 6 level PE numerical models which have been developed over the last three and one-half years by W. Fingerhut. One is 3-D and one axisymmetric. The advective terms are in flux form and an eddy diffusion is utilized. The generalized sigma is used as the vertical coordinate. The tropopause, top of the boundary layer, and the earth's surface are all coordinate surfaces as shown in Fig. 4. One can visualize this system as three models (stratosphere, troposphere, and boundary layer) where the boundary conditions are matched.

The upper-most layer is thought of as a model stratosphere. It is stable and, therefore, resists deformation. This effect is very important if upper-tropospheric and surface pressure gradients are to respond realistically to tropospheric heat sources.

		$P(t=0)$	σ
—————	$\phi, \pi\sigma = \omega = 0$	80 mb	-2
—————	$\phi, P, \pi\dot{\sigma} = 0$	120	-1
—————	$\phi, \pi\dot{\sigma}$	288	-.8
—————	$\phi, \pi\dot{\sigma}$	456	-.6
-----	$\pi u, \pi v, \pi T, \pi q, \omega$		
—————	$\phi, \pi\dot{\sigma}$	624	-.4
—————	$\phi, \pi\dot{\sigma}$	792	-.2
—————	$\phi, P, \pi\dot{\sigma}$	960	0
—————	$\phi = 0, P, \pi\dot{\sigma} = 0$	1010	1

Fig. 4. Vertical structure of the model and the vertical distribution of variables. Variables at half levels are only illustrated once.

The boundary layer is treated as a mixed layer. A frictional stress is computed at the earth's surface and assumed to decrease linearly to zero at the top of the layer.

Centered differences are used both in space and time. One time-step of the 3-D model requires about .7 seconds on the CDC 7600. The 2-D model uses about .02 seconds per time step.

We have many experiments planned focussing on the dynamics of tropical weather systems, particularly the cloud cluster. We feel that we are in a very favorable position to perform realistic numerical simulations due to the availability of detailed observations obtained

by the weather system compositing research studies referred to in Table 1. We are planning to investigate the topics of tropical weather system maintenance, diurnal variation, and tropical storm genesis. The latter subject has yet to be properly treated in numerical model simulations. All previous studies have dealt with the intensification of an existing closed vortex, with very large low-level vorticity values, into a tropical cyclone. Such vortices normally intensify when located over warm tropical waters. The crucial question is how these relatively rare vortices form initially. More complete discussions of this topic are presented in Gray (1975a) and Zehr (1976).

A crucial step in the first area of investigation was the diagnosis of the cumulus forcing in the cluster. We define this as the sum of the vertical advection, condensation, and evaporation terms in the temperature equation. Unlike nearly all existing investigators, we refer to the vertical temperature advection as a cloud term since nearly all the upward vertical motion in convective areas takes place in clouds and not in the environment. Further, this term is very large as is the sum of the condensation and evaporation terms. However, the sum of all cloud terms is very small and, therefore, easier to deal with. Condensation energy release is directly tied to upward vertical motion. It typically does not bring about direct environmental sensible temperature gains but goes primarily into potential energy gains (Gray, 1973). The troposphere experiences warming due to condensation only as a consequence of compensating dry adiabatic sinking motion (Lopez, 1973). Much of this compensating sinking motion occurs at locations removed from the cloud areas. The subsidence warming occurring within the cloud areas is largely expended

TABLE 1

Recently Completed and Current Tropical Cyclone Research Projects

<u>Completed Studies</u>	<u>Subject</u>	<u>Region</u>	<u>Data Set</u>
(Shea and Gray, 1973)	Inner Core Structure	N. Atlantic	NOAA flight data 1957-67
(Gray and Shea, 1973)	Inner Core Structure	N. Atlantic	" " "
(Gray and Shea, 1976)	Data Summary of NOAA's Hurricane Inner-core Radial Leg Flight Penetrations 1957-1967, 1969	N. Atlantic	" " "
Gray, (1975a, 1975b)	Tropical Cyclone Genesis	Global and N.W. Pacific	Numerous Climatological Sources
Frank, 1976	Tropical Cyclone Structure and Energetics	N.W. Pacific	~18,000 Rawinsonde Soundings (1961-1970)
George, 1975	Tropical Cyclone Motion	N.W. Pacific	~18,000 Soundings (1961-1970)
Zehr, 1976	Tropical Cyclone Genesis	N.W. Pacific	~20,000 Soundings (1961-1970)
Current Tropical Cyclone Research Studies			
<u>Subject</u>	<u>Region</u>	<u>Data Set</u>	
1) Structure	N. Atlantic	Soundings from 1956-75	
2) Motion	N. Atlantic	" " "	
3) Genesis	N. Atlantic	1956-1975 Soundings	

TABLE 1 (cont'd)

<u>Subject</u>	<u>Region</u>	<u>Data Set</u>
	N.W. Pacific	1961-1970 Soundings (Pacific data set is being expanded to 20 years)
	N.W. Pacific	DMSP Data
4) Intensity Change	N. Atlantic N.W. Pacific	Same as 3) Genesis
5) Satellite Applicability	N.W. Pacific	DMSP (1971-1975)
6) Numerical Modeling of Tropical Cyclone Genesis		

in balancing the cloud region liquid water reevaporation due to cloud detrainment. Williams and Gray (1973) and Ruprecht and Gray (1976) have demonstrated that the direct influence of the typical 4° diameter cluster condensation (equivalent to $1000-1500 \text{ calories/cm}^2$ per day) on cluster sensible temperature change is nearly zero. Cluster cumulus clouds typically exert only a very small sensible heat change upon the cluster itself. Most cumulus condensation energy is exported to the surrounding regions to balance the outer subsidence.

We believe it is important to point out that the net effect of all the cloud induced temperature changes is much less than the clear atmosphere net radiative cooling. Radiational forcing appears to be larger than that of cumulus convection in the organized tropical cloud cluster. This has broad implications for other modeling work.

Our work on the modeling of the diurnal variation of the cluster is well under way. We have reproduced the large diurnal variations in rainfall rates and divergence profiles which were observed by Jacobson and Gray (1976). This shows a significant diurnal variation. We have also noted two ways in which the diurnally varying radiation affects the cluster. The obvious one is through the time varying radiative cooling of the surrounding clear environment. However, the energy gain during the day (loss at night) from cloud tops in the cluster is equally important. Both influence the hour of maximum rainfall and the character of the cluster inflow profile.

Summary of Recent and Current Research Projects. Table 1 shows the tropical cyclone research projects which are either now in progress or have been completed since 1972 at CSU. The more important findings of these studies are summarized in the following chapters. Many of the

results presented in this report have applicability to forecasting and numerical modeling.

3. TROPICAL CYCLONE MOTION

Steering Flow. The N.W. Pacific rawinsonde compositing study by George (1975) revealed strong correlations between the direction and speed of storm motion and the area weighted average flow from $1-7^{\circ}$ radius. It was found that tropical cyclones move about 16° to the left of the average $1-7^{\circ}$ flow at 500 mb. Their speeds of movement average 1.16 times the speed of the $1-7^{\circ}$ wind at 700 mb. Other radial bands and vertical levels did not give such consistent results.

The above values are not merely the result of averaging many storms with greatly different storm motion-surrounding flow relationships. The data were divided into 13 stratifications according to latitude, speed and direction of movement, intensity and intensity change. Twelve of these stratifications are independent subsets of the typhoon data set (all soundings with central pressures $P_c \leq 980$ mb), and the remaining data set ($980 < P_c \leq 1000$ mb) is completely independent of the others. The stratifications and their storm motion-surrounding flow relationships are summarized in Table 2. The storm direction varied only from $12-23^{\circ}$ left of the averaged 500 mb wind. Storm speed was always from 1.07 to 1.24 times the 700 mb winds. These relationships are remarkably consistent considering the independence of the data subsets and the wide variety of storm types encompassed. Cyclones moving in various directions and at different speeds behave similarly.

Steering flow was also investigated for winds averaged through various vertical levels. Table 3 shows the best results for the same 13 stratifications shown in Table 2. The most consistent correlation with direction of storm motion was found for the 700-500 mb layer winds while storm speed fit the 100-500 mb averaged winds best. In both cases

TABLE 2

HORIZONTAL MULTIPLE RADIAL BAND SUMMARY FOR 1-7° BAND

Stratification	Mean Storm Direction	Mean 1°-7° Surrounding Wind Direction at 500 mb	Storm Deviation from Surrounding Wind (L-Left)	Mean Storm Speed (ms ⁻¹)	Mean 1°-7° Surrounding Wind Speed at 700 mb (ms ⁻¹)	Ratio Storm Speed/Surrounding 1-7° Wind Speed
<u>Latitude</u>						
Latitude >20°N	352°	010°	18°L	5.61	5.06	1.11
Latitude <20°N	300°	314°	14°L	5.05	4.23	1.19
<u>Speed</u>						
Slow Storm Speed 0-3 ms ⁻¹	338°	001°	23°L	2.43	2.19	1.11
Moderate Storm Speed 3-7 ms ⁻¹	326°	344°	18°L	5.19	4.37	1.19
Fast Storm Speed >7 ms ⁻¹	006°	018°	12°L	10.12	8.71	1.16
<u>Direction</u>						
Direction A 250° < Dir. ≤ 310°	285°	300°	15°L	6.16	4.96	1.24
Direction B 310° < Dir. ≤ 350°	324°	341°	17°L	5.32	4.39	1.21
Direction C 350° < Dir. ≤ 060°	027°	042°	15°L	7.08	6.59	1.07
<u>Intensity</u>						
Intensity 1 1000mb ≥ C.P. > 980mb	319°	331°	12°L	4.87	4.07	1.20
Intensity 2 980mb ≥ C.P. > 950mb	326°	343°	17°L	5.03	4.22	1.19
Intensity 3 C.P. ≤ 950mb	319°	341°	22°L	5.17	4.34	1.19
<u>Intensity Change</u>						
Deepening Storms	304°	317°	13°L	4.89	4.31	1.13
Filling Storms	360°	017°	17°L	5.69	5.13	1.11
Mean: 16.4°L.				Mean: 1.16		
Standard Deviation: 3.4°				Standard Deviation: 0.05		

TABLE 3

VERTICAL MULTIPLE RADIAL BAND SUMMARY FOR 1-7° BAND						
Stratification	Mean Storm Direction	Mean 1°-7° Surrounding Wind Direction (700-500 mb)	Storm Deviation from Surrounding Wind	Mean Storm Speed (ms ⁻¹)	Mean 1°-7° Surrounding Wind Speed (1000-500 mb) (ms ⁻¹)	Ratio Storm Speed/Surrounding 1-7° Wind Speed
<u>Latitude</u>						
Latitude >20°N	352°	007°	15°L	5.61	4.55	1.23
Latitude <20°N	300°	312°	12°L	5.05	4.05	1.25
<u>Speed</u>						
Slow Storm Speed 0-3 ms ⁻¹	338°	359°	21°L	2.43	1.91	1.27
Moderate Storm Speed 3-7 ms ⁻¹	326°	342°	16°L	5.19	4.03	1.28
Fast Storm Speed >7 ms ⁻¹	006°	017°	11°L	10.12	7.77	1.30
<u>Direction</u>						
Direction A 250° < Dir. ≤ 310°	285°	302°	17°L	6.16	4.65	1.32
Direction B 310° < Dir. ≤ 350°	324°	337°	13°L	5.32	4.25	1.25
Direction C 350° < Dir. ≤ 060°	027°	040°	13°L	7.08	5.67	1.25
<u>Intensity</u>						
Intensity 1 1000mb ≥ C.P. > 980mb	319°	333°	14°L	4.87	3.71	1.31
Intensity 2 980mb ≥ C.P. > 950mb	326°	344°	18°L	5.03	3.87	1.29
Intensity 3 C.P. ≤ 950mb	319°	340°	21°L	5.17	4.03	1.28
<u>Intensity Change</u>						
Deepening Storms	304°	318°	14°L	4.89	3.82	1.28
Filling Storms	360°	019°	19°L	5.69	4.55	1.25
Mean: 15.7°L				Mean: 1.27		
Standard Deviation: 3.3°				Standard Deviation: 0.03		

area weighted averaged winds from $1-7^{\circ}$ were found to give the most consistent results.

The storm motion-surrounding flow relationships were essentially similar when geostrophic winds computed from the observed heights were used instead of observed winds. This indicates that height and wind fields may be used interchangeably for storm motion forecasting according to operational convenience.

The relationships between storm motion and the winds in the octant to the right of the direction of storm motion were investigated. It was found that the right octant winds at 850 mb at all radii from 1° to 9° were within about 5° of the mean storm direction for all stratifications. There were no good correlations between right octant winds and storm speed.

Further steering flow analyses are being performed for N. Atlantic tropical cyclones to verify the results more thoroughly. A comparison of right vs. left-turning storms is being made to try and separate the factors affecting storm motion from mean environmental flow. Early results indicate that there are some persistent differences in the 200 mb wind fields. Data prior to motion change will be examined to determine if there is a lag time between changes in the wind field and changes in storm motion. If such a lag is found, observations of surrounding winds might allow forecasts of sudden direction changes. In addition, the denser data network in the West Indies may allow studies of the variabilities of individual storm motions rather than groups of storms. This was not possible in the data-sparse N.W. Pacific.

Recurvature. The most crucial problem facing tropical cyclone forecasters is the prediction of recurvature. To analyze the features

of the flow-field associated with recurvature, twenty-one pairs of tropical cyclones were selected. Each pair included one recurving and one non-recurving storm where the tracks prior to recurvature were within 5° latitude of each other. The tracks of the two types of storms are shown in Figs. 5 and 6. A separation point (S) was identified where the recurving storm began to deviate significantly from the non-recurving track. Data was composited for each type of storm (recurving and non-recurving) for various time intervals up to 60 hours before S.

Differences between recurving and non-recurving storms were observed in both the lower and upper troposphere, but upper level differences were far more pronounced. Figure 7 shows composite 200 mb winds for both types of storms and the difference between the two types 60 hours prior to the separation point. The scale of the cylindrical grid has been altered so that the closest plotted point is 8° latitude from the storm center. The westerlies $10\text{--}20^{\circ}$ north of the storm are much stronger and exist closer to the storm center for recurving storms. Note that these large differences occur $2\frac{1}{2}$ days before recurvature. As the storms approach the recurvature point, the westerlies get stronger and closer to the center (Figs. 8 and 9). It has long been known that tropical cyclones tend to recurve under the influence of westerly troughs to the north, but this is the first quantitative analysis showing a strong correlation between upper level winds and recurvature well in advance of the first change of direction. Considerable improvements in forecasting skill may result from careful analysis of upper level winds. Table 4 summarizes the recurving/non-recurving wind, height and temperature differences at 700 mb and 200 mb from 12 hours to 60 hours prior to the separation point.

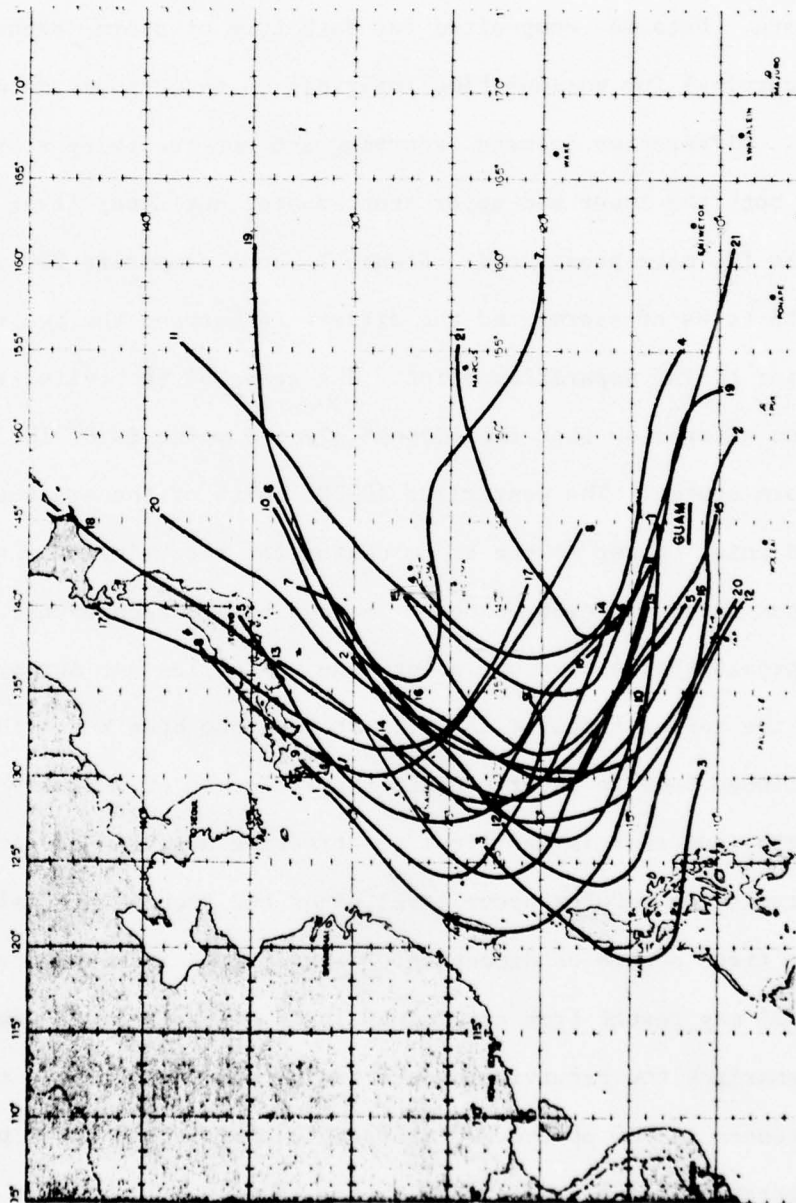


Fig. 5. Actual tracks of the 21 recurring storms.

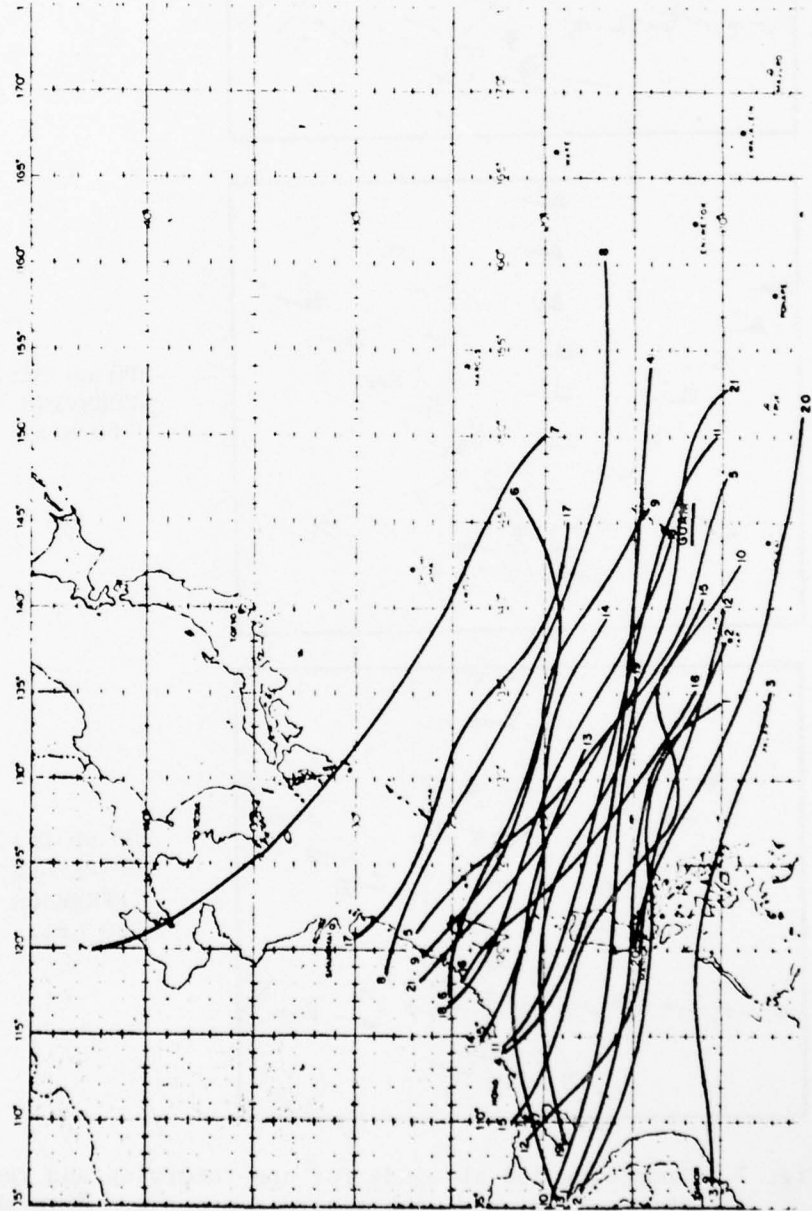
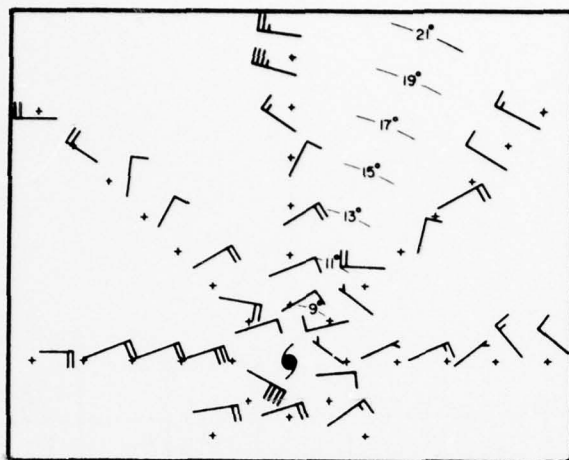
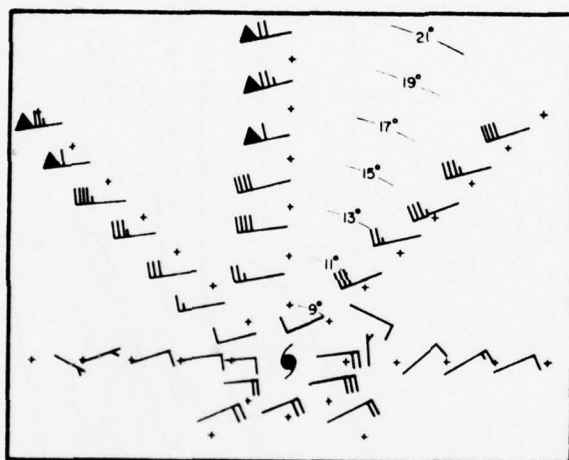


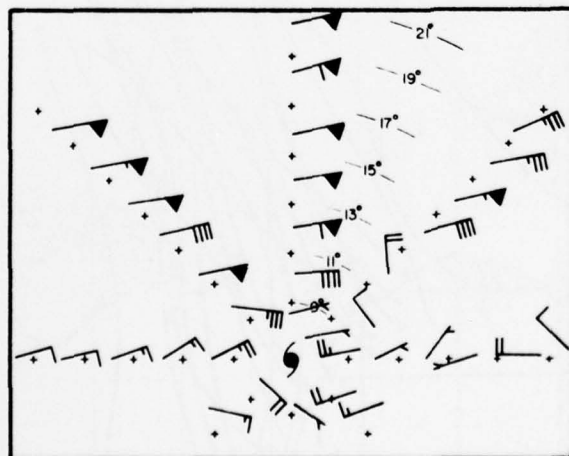
Fig. 6. Actual tracks of the 21 non-recurring storms.



200 mb Dir. & Speed
NON-RECURVING at time
S-60 hrs.

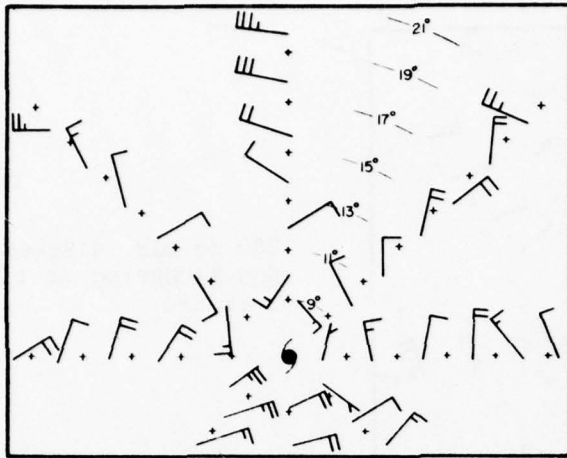


200 mb Dir. & Speed
RECURVING at time
S-60 hrs.

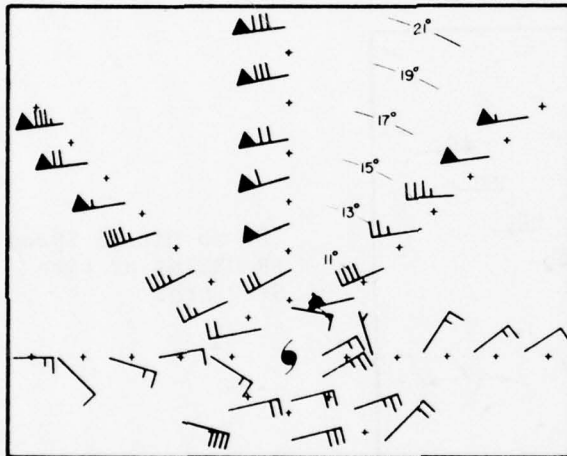


200 mb Dir. & Speed
NON-RECURVING-RECURVING
DIFFERENCE at time
S-60 hrs.

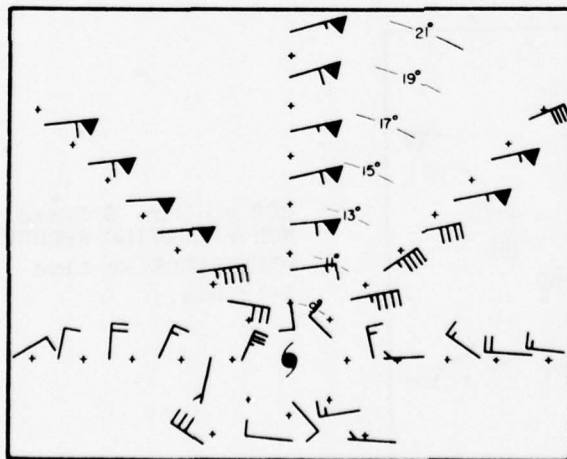
Fig. 7. Composite 200 mb winds for non-recurving and recurving storms 60 hours prior to the separation point. Also shown is the difference between the 2 composites.



200 mb Dir. & Speed
NON-RECURVING at time
S-36 hrs.

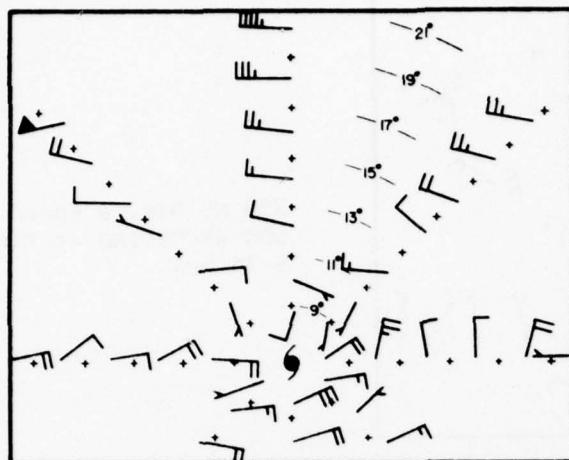


200 mb Dir. & Speed
RECURVING at time
S-36 hrs.

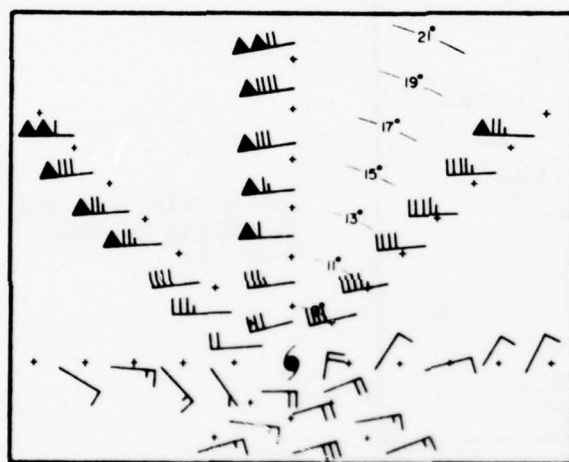


200 mb Dir. & Speed
NON-RECURVING-RECURVING
DIFFERENCE at time
S-36 hrs.

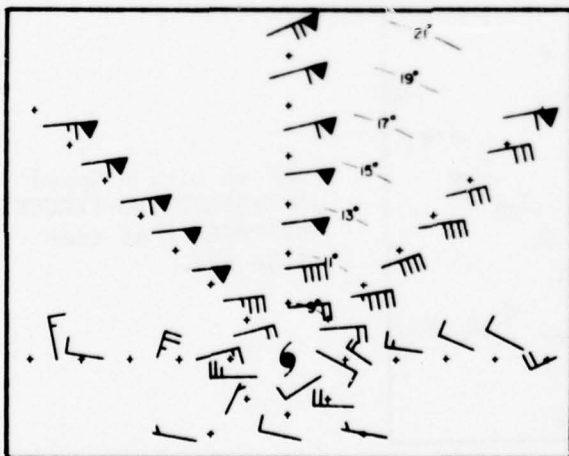
Fig. 8. Same as Fig. 7, except for the (S-36) mean composite time period.



200 mb Dir. & Speed
NON-RECURVING at time
S-12 hrs.



200 mb Dir. & Speed
RECURVING at time
S-12 hrs.



200 mb Dir. & Speed
NON-RECURVING-RECURVING
DIFFERENCE at time
S-12 hrs.

Fig. 9. Same as Fig. 7, except for the (S-12) mean composite time period.

TABLE 4

SUMMARY OF NON-RECURVING MINUS RECURVING PARAMETER DIFFERENCES

Parameter	Data Average 48-72 Hours Prior to Separation (S-60)	Data Average 24-48 Hours Prior to Separation (S-36)	Data Average from Time of Separation to 24 Hours Prior to Separation (S-12)
700 mb zonal wind field	4-8 ms ⁻¹ at 8-12° radius (NW-NE)	4-8 ms ⁻¹ at 8-12° radius (NW-NE)	4-8 ms ⁻¹ at 8-12° radius (NW-NE)
200 mb zonal wind field	20-24 ms ⁻¹ at 14-20° radius (NW-NE)	24-28 ms ⁻¹ at 14-20° radius (NW-NE)	30-36 ms ⁻¹ at 14-20° radius (NW-NE)
700 mb meridional wind field	2-4 ms ⁻¹ at 14-20° radius (NW-N)	2-4 ms ⁻¹ at 8-20° radius (N-NE)	2-4 ms ⁻¹ at 8-16° radius (NE)
200 mb meridional wind field	10-12 ms ⁻¹ at 12-20° radius (NW-N)	12-16 ms ⁻¹ at 12-20° radius (N-NE)	12-14 ms ⁻¹ at 12-20° radius (W-NE)
700 mb height field	40 meters at 16-18° radius (N)	40 meters at 16-20° radius (N-NE)	30 meters at 16-20° radius (N-NE)
200 mb height field	>150 meters at 18-20° radius (NW-N)	>200 meters at 18-20° radius (N)	>300 meters at 18-20° radius (N)
700 mb tempera- ture field	40C at 18-20° radius (NW-N)	6° at 18-20° radius (NW-N)	8°C at 18-20° radius (NW-N)
200 mb tempera- ture field	10C at 18-20° radius (NW-N)	20C at 18-20° radius (NW-N)	20C at 18-20° radius (NW-N)

Current and future recurvature research at CSU is centered on an extension of the above analysis to North Atlantic storms and on establishing individual case variability. It is hoped that an operational forecasting scheme will result. DMSP data are also being analyzed to determine any relationships between storm motion and convective patterns.

Recommendation. Individual case statistics using 200 mb cyclone data should be developed. The middle tropospheric winds at 500 and 700 mb should not be used exclusively to forecast recurvature.

Relationships between changes in storm motion and changes in the surrounding wind and height fields must be explored in more detail. It is extremely important to determine whether there are observable changes in the environment prior to changes in storm direction. The individual variabilities of storm motion with respect to observed environmental features should be analyzed further.

4. INTENSITY CHANGES

Little skill has been developed in the forecasting of tropical cyclone intensity changes. The N.W. Pacific typhoon compositing study (Frank, 1976) was used to examine persistent differences between tropical cyclones with different central pressure (P_c) tendencies. Four data sets were assembled:

- 1) Deepening Typhoons - all storms with $P_c \leq 980$ mb and with central pressures in sustained falling trends,
- 2) Filling Typhoons - all storms with $P_c \leq 980$ mb and with the central pressures in sustained rising trends,
- 3) Developing Tropical Storms - all storms with $980 \text{ mb} < P_c \leq 1000$ mb with falling central pressures and which soon reached typhoon intensity ($P_c \leq 980$ mb), and
- 4) Non-Developing Tropical Storms - storms with $980 \text{ mb} < P_c \leq 1000$ mb which never reached typhoon intensity.

The results are as follows:

Potential Buoyancy. The value of θ_E at the surface minus the saturated θ_E (θ_{ES}) value at 600 mb gives a measure of the atmosphere's potential to sustain deep cumulus buoyant moist convection. Values of $\theta_{E_{sfc}} - \theta_{ES600}$ are plotted for deepening and filling typhoons (Cases 1 and 2) in Figs. 10 and 11. Note that the potential buoyancies to the northwest of the storm centers differ considerably. (The mean direction of storm motion is NNW). Filling storms tend to have large areas of strongly negative buoyant air in this region while deepening storms are closer to neutral buoyancy in these areas. The difference seems to arise from cooler, drier surface air in the filling storms. Similar results are found for developing storms (neutrally buoyant) and non-developing storms (negatively buoyant). Since substantial low level inflow relative to the moving storm center comes from the northwest, it

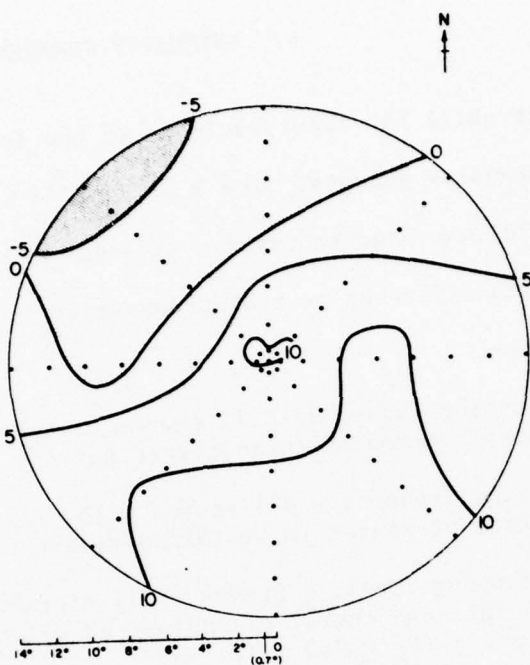


Fig. 10. $\theta_{E_{SFC}} - \theta_{ES_{600\text{ mb}}}$ for deepening typhoons.

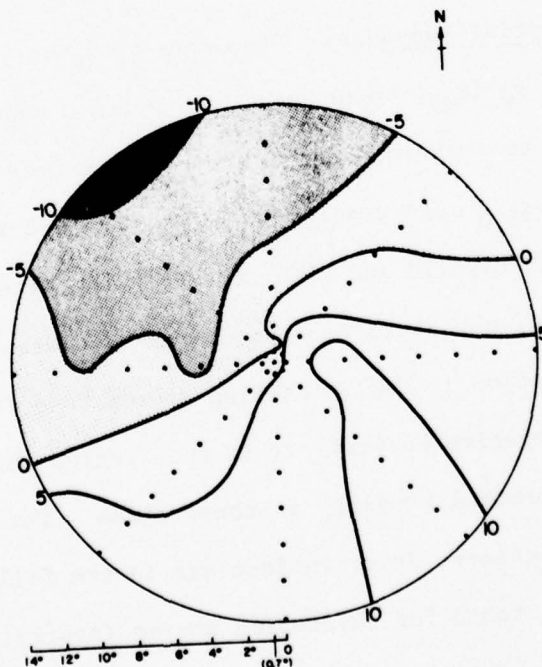


Fig. 11. $\theta_{E_{SFC}} - \theta_{ES_{600\text{ mb}}}$ for filling typhoons.

is clear that the filling and non-developing storms are advecting in low level air which is relatively unfavorable for moist convection. This may be an important influence on the weakening or non-developing storms. Intensifying storms also show somewhat more favorable buoyancy conditions to the south than do weakening storms.

The above results are essentially unchanged when the data is stratified by latitude (North and South of 20°N). However, there are seasonal and latitudinal biases in the data. The percentages of storms occurring in the winter and spring are significantly larger for filling and non-developing storms than for deepening and developing ones. During these seasons the sea surface temperatures to the northwest of the mean storm centers become quite cold. The filling and non-developing storms also tend to be farther north than their intensifying counterparts. It is not clear whether the observed cool, dry low level air is directly responsible for storm weakening. The fact that filling and non-developing storms are relatively more common in winter and at northerly latitudes suggests a correlation, but other factors may be important or dominant. The above study does lend some support to the hypothesis that storms tend to weaken as they move over cold water as discussed by Brand (1971).

Upper Tropospheric Trough. A strong upper level (300-100 mb) trough has been observed in composites of filling and non-developing storms. The trough, maximum at 200-150 mb, is observed at large radii ($10-14^{\circ}$) to the northwest of the storm center. It can be determined from both the height and wind fields. Figures 12 and 13 show the 150 mb height and wind fields for deepening and filling storms, respectively. The trough is cold core. It is related to numerous factors which might cause intensity changes including the low-level stability and the characteristics of the upper-level outflow.

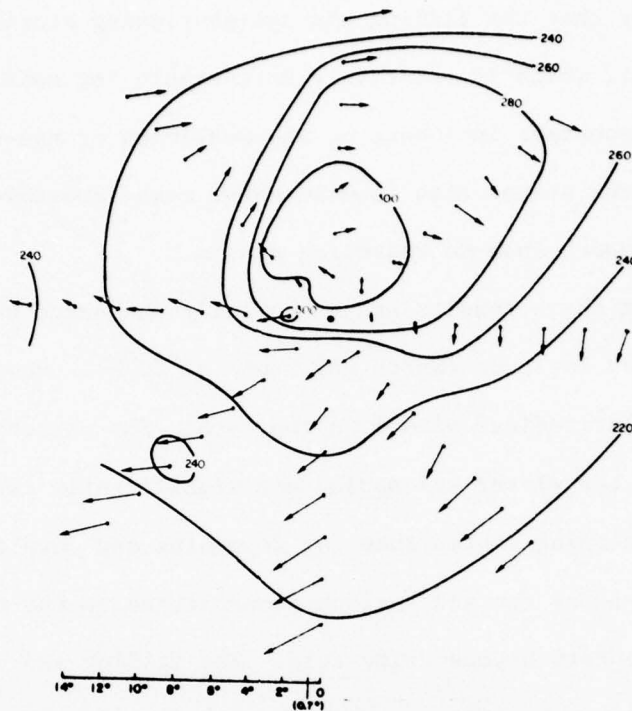


Fig. 12. 150 mb height and wind fields for deepening typhoons. Height units = 14, - - - meters.

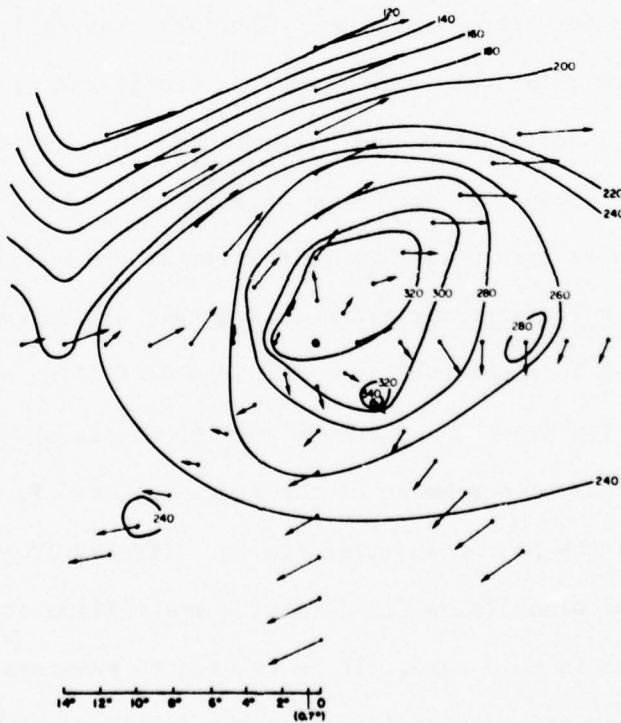


Fig. 13. 150 mb height and wind fields for filling typhoons. Height units = 14, - - - meters.

Outflow. Typhoon outflow at large radii ($8-14^{\circ}$) is typically concentrated in channels. Upper level (150 mb) outflow for deepening typhoons is maximum to the southwest. Very little outflow is observed to the northeast. However, the composite for filling typhoons shows a maximum outflow toward the northeast with a weaker channel to the southwest. These patterns are evident in Figs. 12 and 13. When the data are further stratified by latitude (north and south of 20°N) the results are similar except that the southwest outflow channel for filling storms south of 20° is stronger than their northeast channel. Similar but less conclusive differences are seen in the composite wind fields for developing vs. non-developing storms. The northeast outflow for filling storms is related to the composite trough seen in Fig. 13. These results contradict those of the recent satellite studies by Ramage (1973) and Tsui *et al.* (1977) which reported strong cirrus outflow to the northeast of deepening storms. This could result from a poor correlation between maximum outflow at outer radii with cirrus cover. However, the Tsui study showed that a cirrus outflow stream was correlated with previous intensification, not current intensity tendency, and Ramage studied only a few cases. It is possible that storms intensify prior to interaction with a westerly trough and then weaken as it approaches as suggested by Riehl (1972).

The physical mechanisms linking outflow characteristics to intensity change are not known. They are probably related to greater angular momentum and kinetic energy exports in the filling systems or to changes in the thermodynamic fields such as extra temperature and moisture ventilation. Current research is concentrating on this subject. Individual case studies will be performed to determine how well northeast outflow jets predict storm weakening on a case by case basis.

Convection as Observed by DMSP Satellite Data. Studies of the amounts of deep convection surrounding deepening and filling storms using DMSP photographs show only slight differences. The deepening storms tend to have slightly more deep convection, but the differences are much too small to be useful on an individual case basis. Studies of the relationship between convective organization and intensity change are planned for the immediate future.

Summary. It is extremely difficult to predict storm intensity changes. The differences between weakening and intensifying storms are small and are usually obscured by large inter-storm variabilities. However, a few differing characteristics are noted. Tropical cyclones tend to weaken as they approach low level cold dry air - usually associated with cold water. In the mean an upper level trough to the northwest and an outflow jet to the northeast are indicative of typhoon weakening or of non-intensification of a tropical storm ($980 < P_c \leq 1000$ mb). No obvious correlation between the amounts of deep convection and intensity tendency are observed.

Future Research. The primary factor limiting composite studies of tropical cyclone intensity changes is an insufficient number of storm cases in each group. The Pacific data set is being expanded to 20 years doubling the size of that sample, and a 20 year data set is also being assembled for the West Indies. It is anticipated that the combined data from these two data sets will allow more quantitative analyses of the processes causing storm intensity changes. In addition, the larger data set will allow stratification of storms into more specific groups. Storms undergoing intensity change may be further stratified by season, latitude, rate of central pressure change, current intensity, etc. This will be a prime topic of future research.

5. TROPICAL CYCLONE GENESIS

The climatological conditions favorable to the formation of tropical cyclones have been summarized by Gray (1968, 1975a), but the physical processes which occur are not well documented. It is known that they develop from rather ordinary looking cloud clusters or disturbances. However, no clear differences between common ordinary clusters and relatively rare pre-typhoon clusters have been observed.

Zehr (1976) compared 10 years (1961-1970) of N.W. Pacific rawinsonde data around clusters which developed into typhoons with data computed from two years of clusters which did not intensify into cyclones. He examined ITCZ clusters only (latitude $5-18^{\circ}$ N). Trade genesis at higher latitudes was not treated. Overall the clusters were very similar, but some significant differences were found.

In this study stage 0 refers to all ITCZ clusters which did not develop into tropical cyclones. Stage 00 is restricted to the months of June-September and to longitudes from 125° E to 165° E. Stage 2 refers to pre-typhoon clusters at all time periods up to 1 day prior to the first aircraft reconnaissance observation (usually about 30 knots maximum wind). The most relevant comparison of developing to non-developing clusters is between stages 00 and 2 since the stage 00 set is more representative of tropical cyclone season and locations than the stage 0 set.

The same subject is being investigated using DMSP satellite photographs to analyze convective differences (Erickson, 1977). The more important results of both studies are discussed below.

Divergence and Vertical Motion. Developing clusters (stage 2) tend to have more convergence/divergence at 4° radius and a greater maximum

upward vertical motion ($\bar{\omega}$) than non-developing clusters (stage 0 and 00), (Figs. 14 and 15). The difference in $\bar{\omega}_{\max}$ is about 25%. This implies more convection in the developing clusters and is in good agreement with the DMSP study showing more deep convection from $0-4^\circ$ for such clusters. Most of the increased convection observed in developing clusters occurs between 2° and 4° radius. There is little difference between the amounts of mean convection in the center region ($0-2^\circ$). Unfortunately, individual clusters are so variable that storm genesis is probably not reliably predictable from observations of amounts of cluster convection.

Low Level Vorticity. It is well known that tropical cyclones tend to form in regions with strong low level vorticity such as the ITCZ (Sadler, 1967; Gray, 1975a). The 900 mb relative vorticity fields of the mean pre-typhoon cluster and of the non-developing cluster data sets are shown in Fig. 16. Note that the area with values greater than $2 \times 10^{-5} \text{ sec}^{-1}$ is significantly larger for the pre-typhoon cluster. In the immediate vicinity of the cluster, the relative vorticity is about twice as large with the pre-typhoon cluster as with the non-developing clusters. This is the most substantial difference between non-developing and pre-typhoon cloud clusters. It may be possible to determine a minimum threshold value of low level vorticity over a $\sim 4^\circ$ radius area for tropical cyclone genesis. The problem is to determine accurate mesoscale vorticities from the limited data available over the tropical oceans. Perhaps satellite determined winds could be used. For example, an observed "sharpening" of the ITCZ suggests locally high values of low level vorticity. The use of vorticity observations as a genesis prediction tool is currently being investigated.

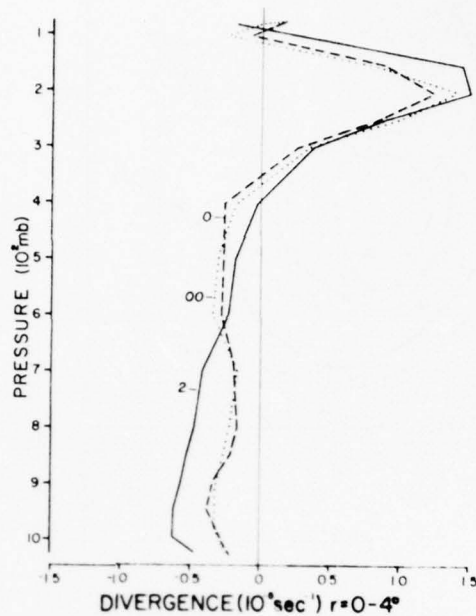


Fig. 14. Mean divergence within the $r = 0-4^\circ$ area for the pre-typhoon cluster (2) and the non-developing clusters (0) and (00).

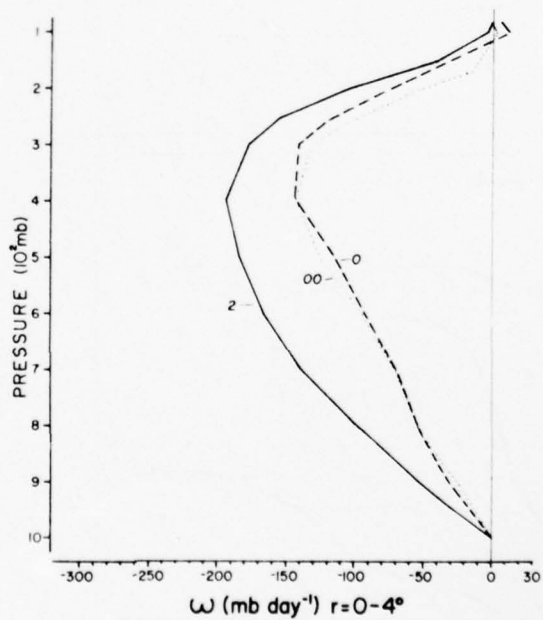
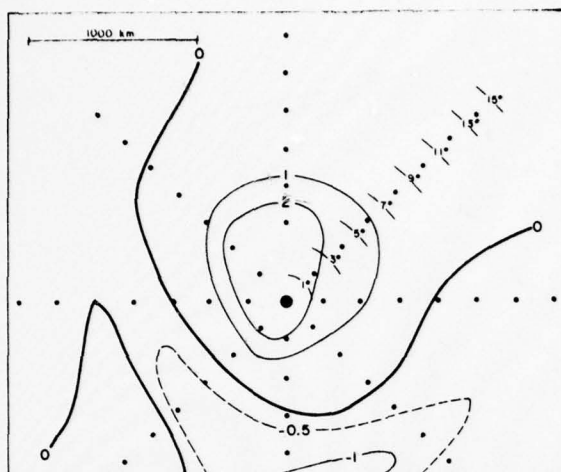
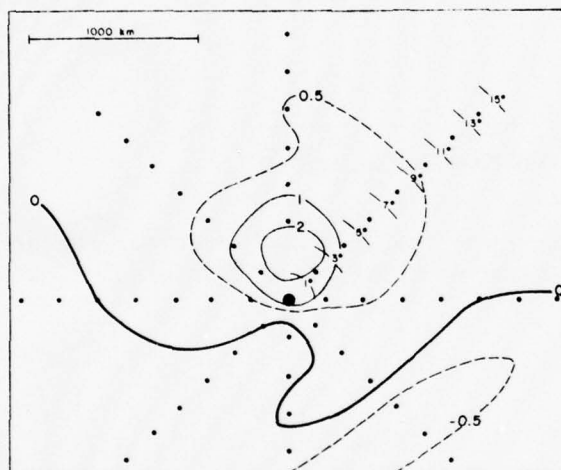


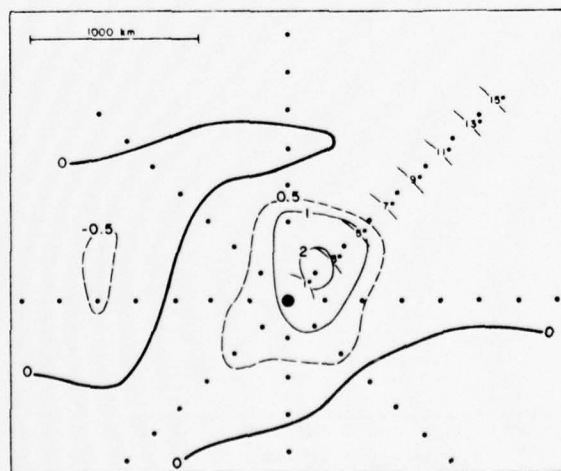
Fig. 15. Mean vertical velocity (ω) in the $r = 0-4^\circ$ area for the pre-typhoon cluster (2) and the non-developing clusters (0) and (00).



Pre-typhoon cluster
(Stage 2)



Non-developing cluster
(Stage 0)



Non-developing cluster
(Stage 00)

Fig. 16. 900-millibar relative vorticity (units are 10^{-5} sec^{-1}).

Vertical Temperature Structure. Developing clusters tend to be slightly warm core in the lower troposphere even at the earliest observation time while non-developers are cold core at those levels (first noted by Riehl in the 1940's). Figure 17 compares the temperature anomalies of both types of clusters. Assuming approximate thermal wind balance, the mean tangential wind profiles should show different vertical gradients of V_T . This proves to be the case (Fig. 18). The developing clusters have maximum cyclonic flow in the lowest levels while non-developing clusters have maximum V_T in the middle levels.

The small temperature anomalies in clusters are very hard to observe for individual cases due to the relatively large inter-sounding variabilities. However, observation of the vertical tangential wind shear holds some promise as a tropical cyclone genesis forecast aid, especially since the warm core is observed at the earliest stages of development.

Anticyclonic Outflow. The 200 mb outflow is more anticyclonic for developing than for non-developing clusters as shown in Table 5. Satellite determined winds should be plentiful enough at this level to allow determination of mean V_T values at various radii.

TABLE 5

Mean Tangential Wind at 200 mb
(m sec⁻¹)

Date Set	$r = 2^\circ$	$r = 4^\circ$	$4 = 6^\circ$
Non-developing (Stage 00)	-1.35	-1.95	-1.09
Non-developing (Stage 0)	-0.70	-0.66	-1.25
"Pre-typhoon" (Stage 2)	-1.18	-1.72	-2.90

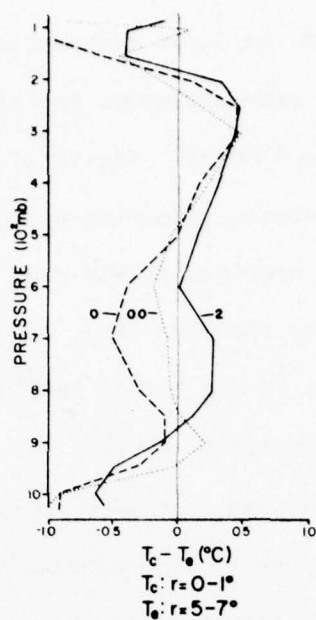


Fig. 17. Vertical temperature profiles: pre-typhoon cluster (2) versus non-developing clusters (0 and 00). T_c = mean temperature of the cluster. T_e = mean temperature of the surrounding region. $T_c = r = 0-1^\circ$, $T_e: 5-7^\circ$.

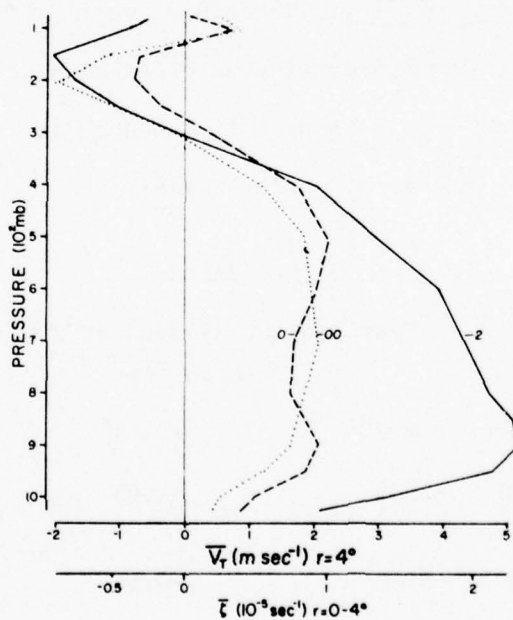


Fig. 18. Vertical tangential wind profiles of the pre-typhoon clusters (2), and non-developing clusters (0 and 00). The mean tangential winds shown are the mean in the $r = 3-5^\circ$ band, and can be interpreted as a mean relative vorticity within $r = 4^\circ$.

Vertical Shear and Ventilation. Strong vertical wind shear is unfavorable for storm development (Gray, 1973, 1968). Figure 19 shows that the zonal vertical shear is less for developing clusters (stage 2) than for non-developers (stage 00). The weak mean vertical shear for stage 0 apparently results from the cancellation of many strong shears of opposite signs. Also shown are the propagation speeds of the clusters.

The radial wind flow relative to the cluster can be analyzed in terms of its divergent and non-divergent ("ventilative") components at the approximate cluster perimeter-- $r = 4^{\circ}$ (Zehr, 1976). The divergent component is merely the absolute value of the mean radial wind ($|\bar{v}_r|$), and the ventilation (VEN) is given by: $VEN = |\bar{v}_r| - |\bar{V}_r|$. Figure 20 shows the mean divergent and ventilative components of the radial wind for both types of clusters. It is clear that ventilation is strongest in the non-developing clusters. Ventilation tends to reduce the temperature and moisture anomalies of the clusters.

Summary. Several major facts concerning differences between ITCZ pre-typhoon cloud clusters and non-developing ITCZ clusters have been established. Many of these reinforce the findings and conclusions of previous studies.

- 1) The mean vertical motion is about 25% greater with pre-typhoon clusters than with non-developing clusters when measured within a large (8° diameter) region centered on the clusters. This difference is observed primarily from $2-4^{\circ}$ radius.
- 2) Pre-typhoon cloud clusters are located in regions with mean low-level relative vorticities in the vicinity of the cluster approximately twice as large as those observed with non-developing cloud clusters, i.e. - the ITCZ has stronger horizontal shear.
- 3) The cold-core structure in the 500-800 mb layer, characteristic of non-developing cloud clusters, is not present with pre-typhoon cloud clusters. This feature is further substantiated by the tangential wind and relative vorticity

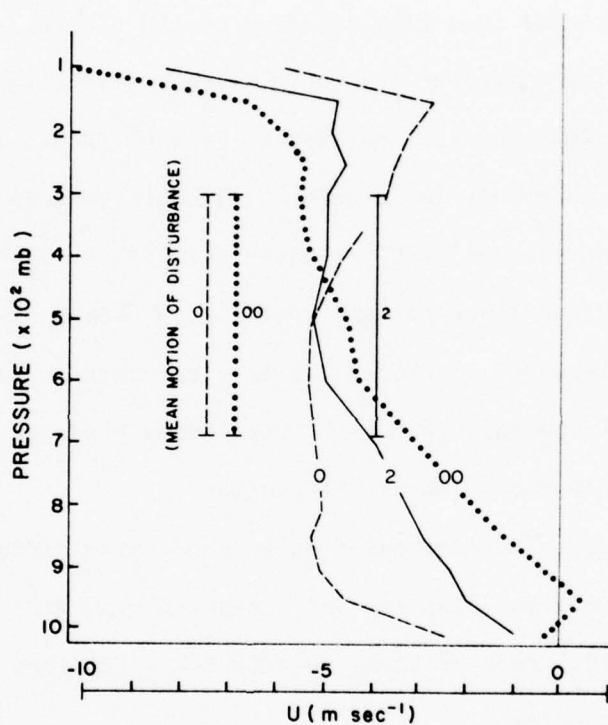


Fig. 19. Zonal wind or u-component of the wind. The mean values of u in the $r = 0-3^\circ$ region are plotted for the pre-typhoon (2) and non-developing (0 and 00) clusters. The mean u-component of the propagation vector is also depicted.

data. The pre-typhoon clusters have a cyclonic wind maximum just above the boundary layer as opposed to a maximum in the middle troposphere for non-developing cloud clusters.

- 4) The outflow in the 150-250 mb layer is more anticyclonic with pre-typhoon cloud clusters than with non-developing clusters.
- 5) In the mean non-developing clusters exist in regions with larger vertical shear of the mean zonal wind although the tropospheric shear of non-developing clusters may still be less than 5-10 m/sec. As a result, the ventilation integrated through the troposphere is greater with non-developing clusters than with pre-typhoon clusters. This inhibits some of the sensible and latent heat accumulations which are favorable for tropical cyclone formation.

It should be stressed that all of the above differences between pre-typhoon and non-developing cloud clusters were noted at a time well before any significant intensification of the pre-typhoon cluster. Mean temperature lapse rates and available buoyant energies were very similar. The observed surface wind speeds averaged less than 5 m sec^{-1} in the immediate area of both the non-developing cluster and the pre-typhoon cluster.

Modeling of Genesis. As previously mentioned, all prior modeling studies of tropical cyclone genesis have started with strong, deep vortices. They have modeled intensification rather than genesis. The transition from a cloud cluster to a deep closed vortex is being studied through modeling research using the 2 and 3-dimensional primitive equation meso-scale models described in Chapter 2.

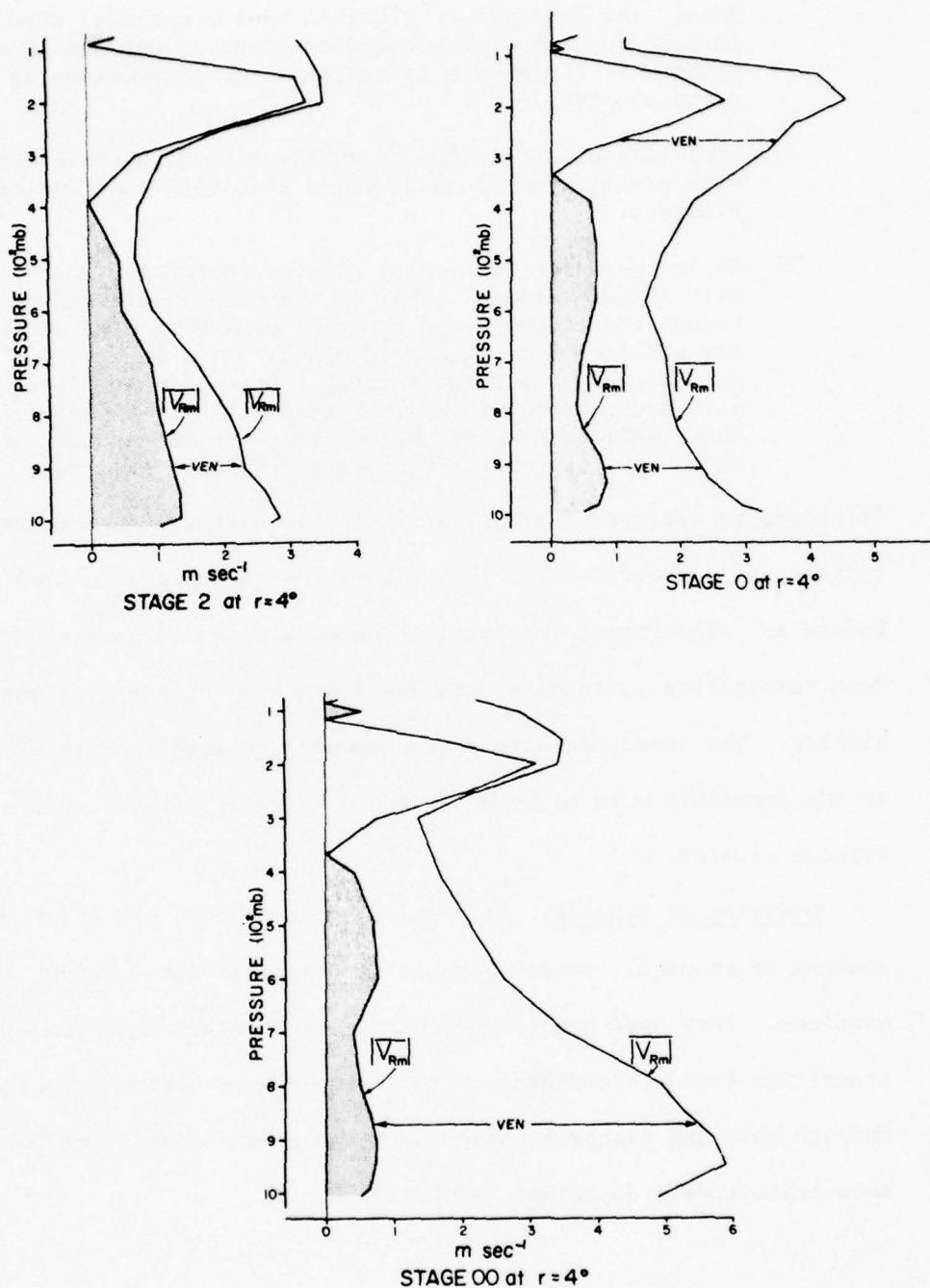


Fig. 20. Vertical profiles of the total mean relative flow ($\overline{V_{Rm}}$), the divergent ($\overline{V_{Rm}}$), and non-divergent (VEN) portions of the flow. Computations are based on the mean relative radial winds at 4° radius. The data sets are: 2, "Pre-typhoon"; 0, non-developing cluster (general); 00, non-developing cluster (restricted).

6. DETERMINATION OF CYCLONE INTENSITY

It is often desirable to know the maximum winds in a tropical cyclone when no aircraft reconnaissance is available. At the present time the only non-aircraft data sources which offer any promise for intensity determination are satellites. One hope for improvement in this forecast area seems to be with establishing a relationship between satellite-observed eye diameter and the maximum intensity. It may also be possible to measure upper level horizontal temperatures and gradients with satellite or aircraft based sensors and thereby infer the low level wind and pressure fields. These topics are being examined by Major C. Arnold at Colorado State University, and preliminary results are presented below.

Observations of Eye Diameter. DMSP photographs of 57 typhoons occurring in the N.W. Pacific from 1971-1975 were examined. There were 276 individual observations, and eyes were visible in 48% of those photographs. Only about $\frac{1}{2}$ of those eyes were sufficiently well defined to allow an estimation of the radius of maximum winds (RMW) which must be determined to estimate maximum wind speeds. Therefore, any estimate of storm intensity based on satellite-observed eye diameter would probably be practical about 1/4 of the time.

Relationship of RMW to Maximum Wind Speed. Shea and Gray (1973) examined the inner-core structure of hurricanes using NOAA flight data. They found a correlation between maximum wind speed and radius of maximum winds (RMW) (Fig. 21), but the variability was so large that individual case predictions would be tenuous. The results are the same when central pressures are compared to satellite-observed eye diameters (Arnold, 1977). The central pressure and maximum winds were also related statistically (Fig. 22), but variability was high. It appears that the only way to estimate storm maximum winds accurately from eye diameter/RMW observations is by using a 2-variable correlation such as

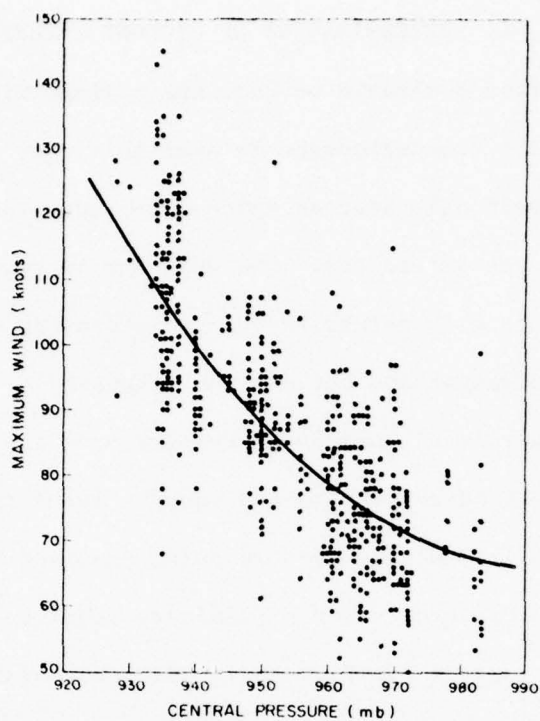


Fig. 21. Variation of the maximum wind with RMW for lower tropospheric data. The best fit curve is indicated by the heavy line.

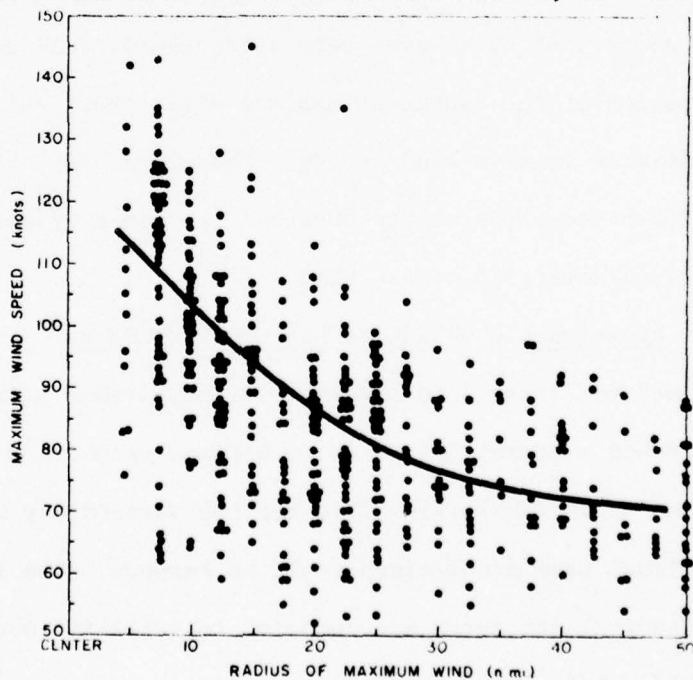


Fig. 22. Variation of the maximum wind with central pressure for all lower tropospheric data. The best fit curve is indicated by the heavy line.

central pressure and RMW or upper level (200-300 mb) temperatures and RMW. This would require measurements of eye temperatures or whatever parameter besides the eye diameter was to be used. At the present time the 2-parameter correlations have not been explored. It is hoped that some method of relating maximum winds to satellite-observed parameters can be developed. Examination of simultaneous satellite and aircraft data is required, and this is planned for the immediate future using 1971-1975 DMSP and aircraft data in the N.W. Pacific.

It should also be noted that maximum winds and central pressures are not necessarily the only storm intensity information of interest. The horizontal extent of strong winds is also crucially important. It is unclear how this parameter could be determined from observations of inner-core characteristics.

Relationship of Intensity to Convection. The current intensity of a tropical cyclone is the cumulative result of all of its previous warming. The total amount of deep convection at any time is not well related to a storm's central pressure or maximum winds. Due to relatively large inter-storm variabilities and diurnal variations in cloudiness, intensity cannot be predicted well in terms of the amount of deep convection observed. There are some relationships between the organization of the convection and storm intensity as reported by Dvorak (1975) and Fett (1966). Banding and symmetry of convection are related to storm intensity. Research into this latter type of intensity determination using satellite data is planned for the immediate future at Colorado State University. It is hoped that by combining rawinsonde observations with the DMSP data, more insight into the relationships between convective organization and inner-storm strength can be obtained.

Determination of Intensity from Upper Level Temperatures. Current research indicates that surface pressures may be estimated from upper tropospheric temperatures (200-300 mb). If this finding is correct, observations of temperatures and temperature gradients at those levels would allow determination of the low level pressure and wind fields. Such temperature measurements could be made from direct aircraft observations or from remote microwave sensors on satellites or high flying aircraft. This is a topic of current research at CSU.

Summary. It may be possible to estimate maximum storm intensity from satellite observations of tropical cyclone eye characteristics at least 1/4 of the time. However, due to the extreme variability of individual storms, it appears that observation of 2 or more parameters is required.

There are no significant correlations between amounts of convection and storm intensity. Research into the relationships between convective organization and storm intensity are planned.

It seems that storm intensity may be determined best from observations of upper tropospheric temperatures using satellite or aircraft based sensors. Research on this topic is underway.

7. CYCLONE STRUCTURE

The recent N.W. Pacific typhoon rawinsonde composite study (Frank, 1976) revealed many features of the structure and energetics of tropical cyclones. Some of the findings which are of particular interest to tropical cyclone modelers are discussed below.

Axisymmetry. Most current tropical storm models are axisymmetric (Kasahara, 1961; Ogura, 1964; Yamasaki, 1968; Ooyama, 1969; Rosenthal, 1970; Sundquist, 1970; and Carrier et al., 1971) although some 3-dimensional models are operational (Anthes et al., 1971; Kurihara and Tuleya, 1974; Mathur, 1975). Many features of the observed storm structure are relatively symmetrical, and horizontal eddy fluxes of sensible heat and water vapor are not too large. However, angular momentum and kinetic energy analyses show very large eddy fluxes of these quantities at outer radii (Figs. 23 and 24). Unless these fluxes can be parameterized, it is doubtful whether an axisymmetric model can be considered realistic. Some of the observed similarities between the circulations of such models and observed tropical storms are probably fortuitous. The eddy generation, dissipation, and export of kinetic energy are all large terms which tend to cancel, but this does not justify their neglect. Eddy momentum fluxes are required to obtain realistic momentum balance in the outflow layer at large radii and to compensate for standing eddies in the Coriolis torque term. Although many features of the tropical cyclone's inner circulation may be modeled adequately in two dimensions, the authors do not believe that such models can yield realistic simulations of the outer cyclone regions.

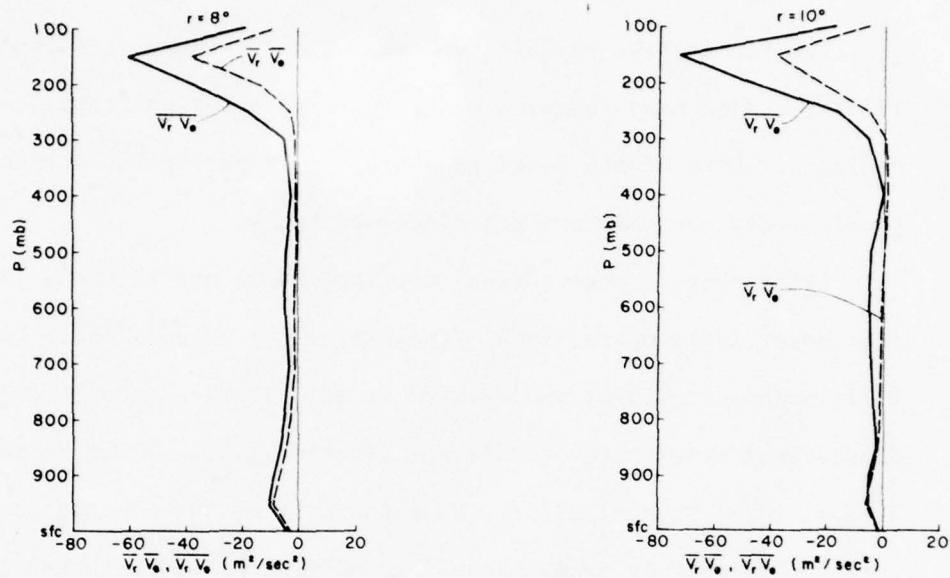


Fig. 23. Total transport of relative angular momentum (divided by radius) and the transport by the mean circulation (dashed line) at $r = 8^\circ$ and $r = 10^\circ$. Negative numbers denote import of momentum.

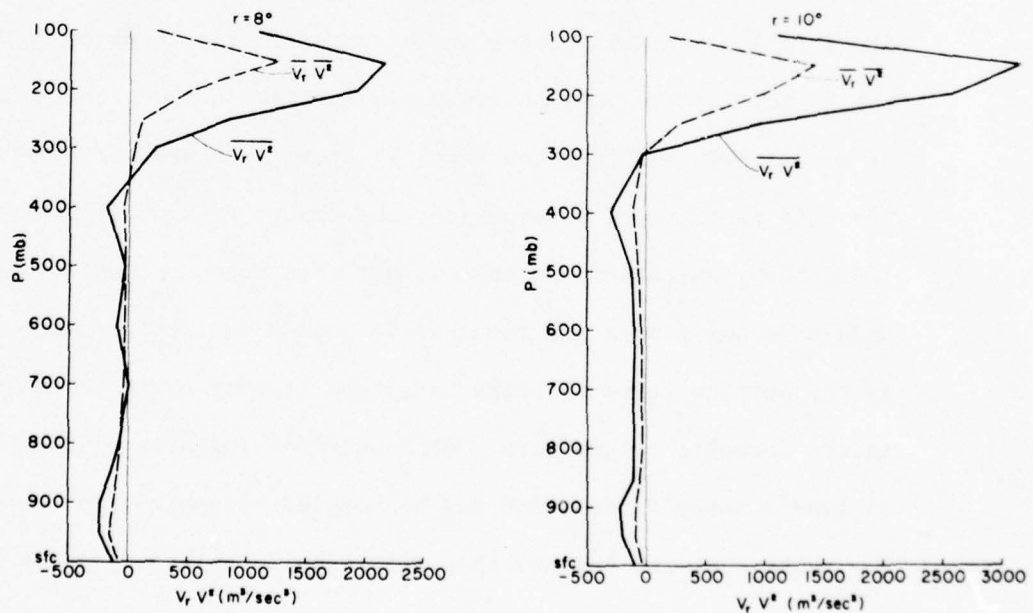
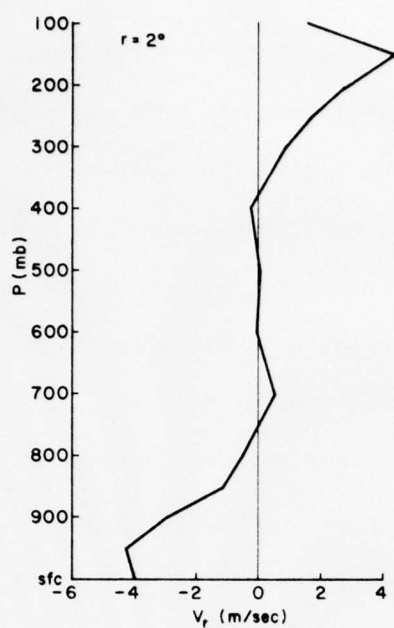


Fig. 24. Total transport of kinetic energy (times 2) and the transport by the mean circulation (dashed line) at $r = 8^\circ$ and $r = 10^\circ$. Positive numbers denote export.

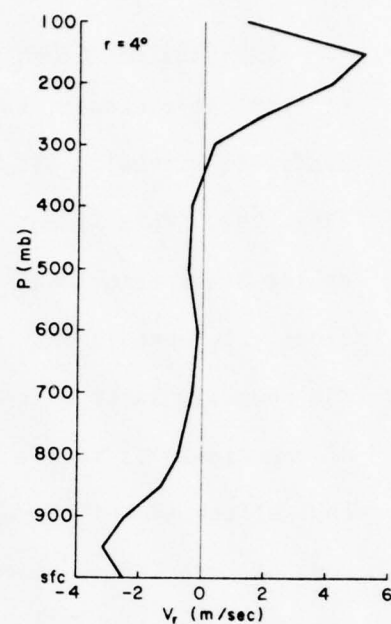
Observed Structure. Several features of the large scale structure of tropical cyclones are particularly important. Although inflow at 2° radius is virtually all below 800 mb, deep inflow exists from 4° outward (Fig. 25). This is not simulated in most models which generally depend on low level frictional convergence alone to force their radial circulations. It appears that most of the middle level inflow subsides into the boundary layer before being cycled upward in clouds. The exact cause of the mid-level inflow is not clear, but this phenomenon has a significant effect on the overall storm moist static energy budget. The magnitude of this inflow casts doubt on the use of CISK as the exclusive forcing mechanism of tropical cyclones. The correlation between vorticity and convergence in the boundary layer is poor, and this also suggests that a reevaluation of the CISK theory is needed.

Soundings (Figs. 26 a-h, Table 6) show more conditional instability at inner radii than usually is assumed, and mid-level humidities are higher than expected. The inner regions show substantial potential for buoyant convection except in the eye. The available data do not show constant vertical profiles of h (or θ_e) or moist adiabatic lapse rates at inner radii. Soundings inside $r = 0.7^\circ$ are based on flight data from Gray and Shea (1973).

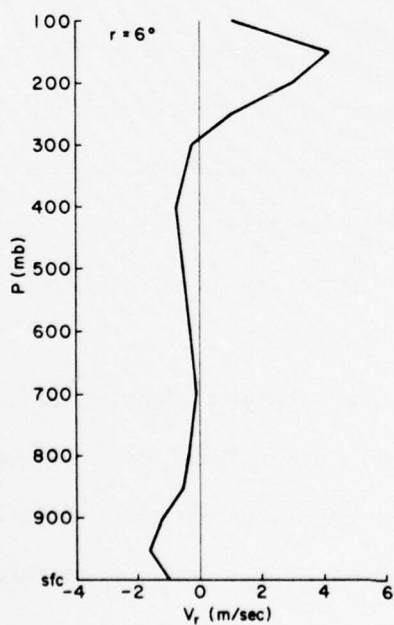
The scale of the circulation is very large. Even at 14° radius there is substantial mean radial flow. Upper level mean and eddy radial fluxes of momentum and kinetic energy are large at outer radii. Although the outer circulation may be independent of the inner core structure, the common assumption of a closed boundary at 1000 km radius or so, does not seem justified.



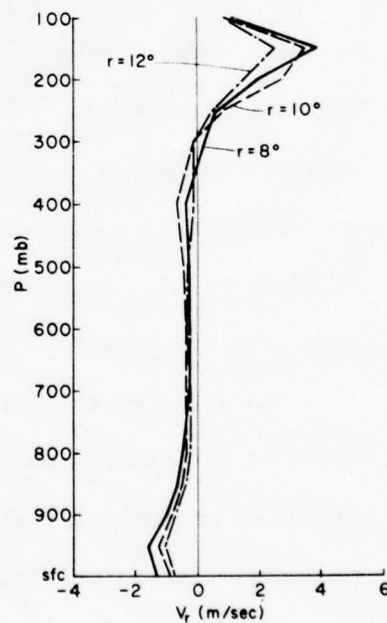
(a) 2-dimensional vertical profile of radial winds (V_r) in m/sec at $r = 2^\circ$.



(b) Same as (a) for $r = 4^\circ$.

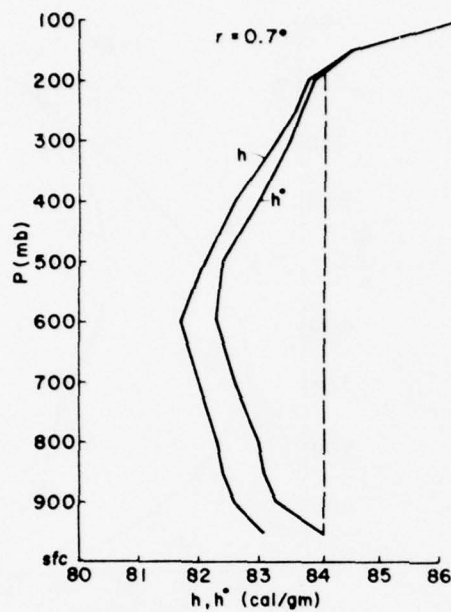


(c) Same as (a) for $r = 6^\circ$.

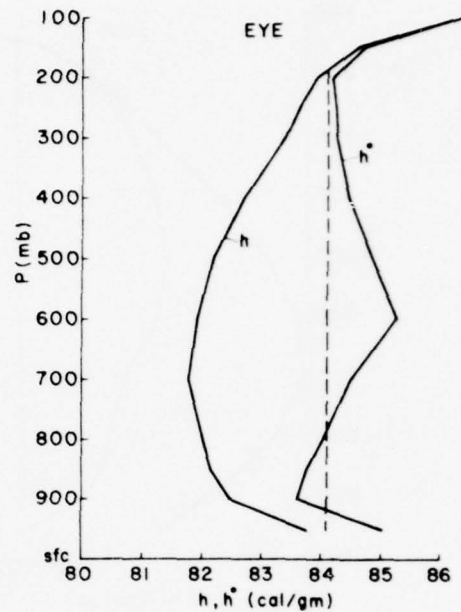


(d) Same as (a) for $r = 8^\circ, 10^\circ$ and 12° .

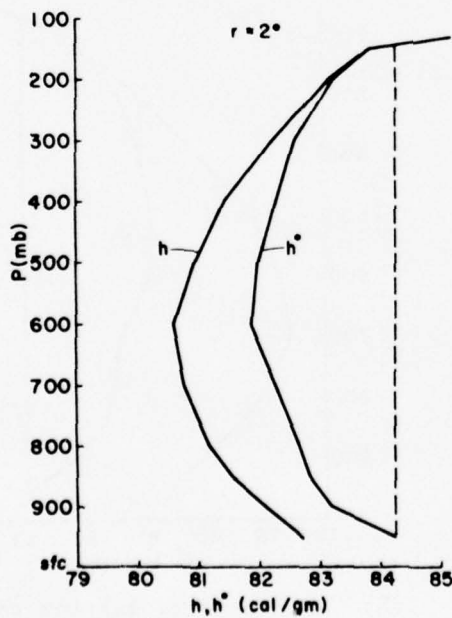
Fig. 25.



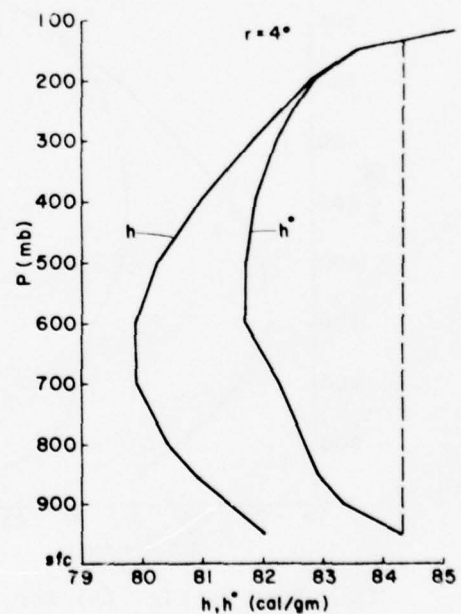
(a) Moist static energy (h) and saturated moist static energy (h^*) at $r=0.7^\circ$. Vertical dashed line is path of undilute saturated ascent from 950 mb.



(b) Same as (a) for eye.



(c) Same as (a) for $r=2^\circ$.



(d) Same as (a) for $r=4^\circ$.

Fig. 26.

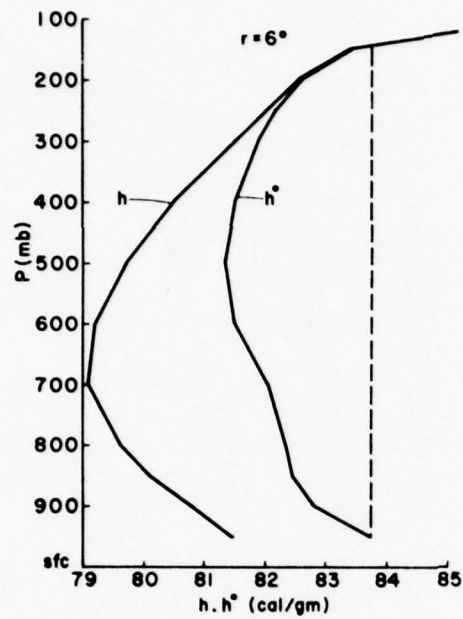
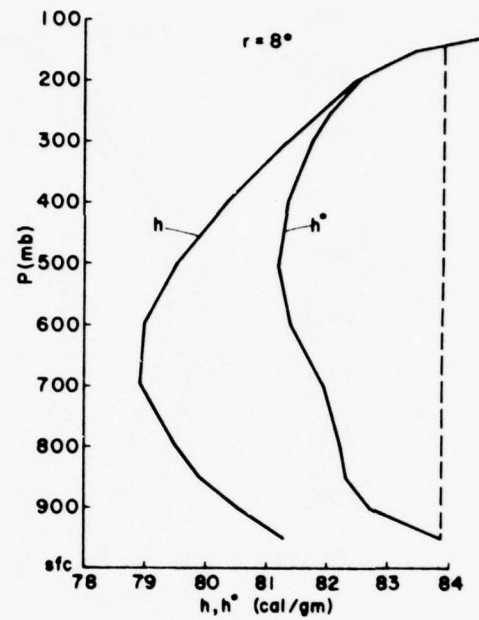
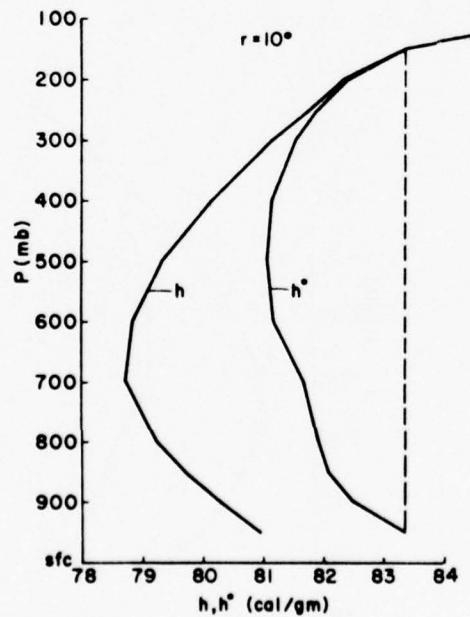
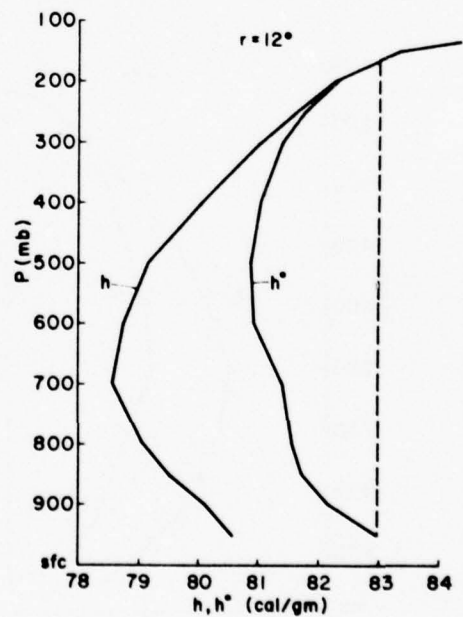
(e) Same as Fig. (a) for $r=6^{\circ}$.(f) Same as Fig. (a) for $r=8^{\circ}$.(g) Same as Fig. (a) for $r=10^{\circ}$.(h) Same as Fig. (a) for $r=12^{\circ}$.

TABLE 6

Mean Soundings $T(^{\circ}\text{C})$ $q \left(\frac{\text{g}}{\text{kg}}\right)$

	Jordan (1958)				NW Pacific (Gray et al., 1975)				eye	$r = 0.7^{\circ}$				$r = 2^{\circ}$					
	Cluster (12Z)		Clear Area		Cluster (12Z)		Clear Area			$r = 0.7^{\circ}$		$r = 0.7^{\circ}$		$r = 2^{\circ}$		$r = 2^{\circ}$			
	T	q	RH		T	RH				T	q	RH		T	q	RH			
sfc	26.3	18.2	84		26.1	88		26.5	--	--	--		24.5	19.4	95		25.7	19.4	90
950	23.0	15.3	81		23.2	87		23.7	24.8	19.2	90		23.8	18.4	94		23.7	17.3	89
900	19.8	13.0	79		20.7	82		20.7	22.1	17.1	89		21.1	16.8	94		20.8	15.7	89
850	17.3	11.0	74		18.2	78		18.1	20.3	15.3	88		18.8	15.3	94		18.4	13.8	87
800	14.6	8.4	68		15.4	77		15.4	18.7	13.8	86		16.7	14.0	93		16.1	12.1	83
700	8.6	5.8	57		9.4	75		9.9	14.3	10.4	80		11.3	11.2	92		10.7	9.1	78
600	1.4	3.6	50		2.0	80		2.3	10.0	7.8	64		5.0	8.2	89		4.1	6.5	76
500	-6.9	2.1	45		-5.7	77		-5.8	2.7	4.7	50		-2.3	6.0	91		-3.2	4.3	70
400	-17.7				-15.8	72		-16.0	-7.2	2.8	50		-11.2	3.5	85		-12.8	2.2	60
300	-33.2				-30.9			-31.3	-21.0	1.2	50		-24.0	1.5	77		-27.0	0.8	53
250	-43.3				-41.3			-41.4	-31.3	.6	50		-33.3				-36.4		
200	-55.2				-54.3			-53.5	-44.5				-46.0				-48.7		
150	-67.6				-69.1			-67.8	-59.8				-60.8				-63.6		
100	-73.5				-77.5			-78.9	-77.1				-77.1				-75.5		
80	-69.8				-72.9			-72.9									-73.6		
70	----																-67.7		
60	-63.9																-64.9		
50	-60.6																-60.9		

TABLE 6 (cont'd)

	$r = 4^{\circ}$			$r = 6^{\circ}$			$r = 8^{\circ}$			$r = 10^{\circ}$			$r = 12^{\circ}$		
	T	q	RH	T	q	RH	T	q	RH	T	q	RH	T	q	RH
sfc	26.1	18.8	85	25.7	17.9	83	25.7	17.7	82	25.5	17.4	82	25.2	17.1	82
950	23.7	16.1	84	23.1	15.3	80	23.2	15.0	78	22.6	14.6	78	22.2	14.1	79
900	20.9	14.5	83	20.2	13.5	80	20.1	13.1	78	19.8	12.8	77	19.4	12.6	78
850	18.4	12.5	79	17.8	11.4	75	17.6	11.1	74	17.3	10.9	73	16.8	10.7	74
800	16.0	10.7	74	15.5	9.5	68	15.3	9.3	67	14.9	9.0	67	14.4	8.9	68
700	10.6	7.6	66	10.2	6.3	57	10.0	6.1	55	9.6	5.9	54	9.2	5.8	55
600	3.7	5.3	64	3.3	4.3	54	3.1	4.0	51	2.7	3.9	50	2.2	3.9	51
500	-3.9	3.3	58	-4.7	2.7	50	-5.1	2.4	46	-5.4	2.3	45	-5.9	2.2	44
400	-14.0	1.7	50	-14.9	1.3	43	-15.4	1.2	40	-15.8	1.1	40	-16.2	1.1	40
300	-28.2	0.6	46	-29.3	0.5	39	-29.9	0.4	35	-30.4	0.4	35	-30.9	0.4	36
250	-38.0			-39.1			-39.6			-40.1			-40.5		
200	-50.2			-51.0			-51.5			-51.8			-52.0		
150	-64.6			-65.0			-65.1			-65.1			-65.1		
100	-76.4			-76.4			-76.2			-75.7			-75.3		
80	-73.4			-74.1			-73.6			-73.1			-72.5		
70	-68.7			-68.6			-68.7			-68.5			-68.3		
60	-65.2			-65.4			-65.3			-65.1			-64.8		
50	-61.1			-61.8			-61.2			-61.3			-61.1		

Cumulus Parameterization. All tropical cyclone models must use some sort of cumulus parameterization scheme to simulate the latent heating processes. The results of this study indicate substantial convection at all radii and large amounts of vertical mass recycling everywhere beyond the eyewall region, especially in the lower troposphere. Figure 27 shows the total upward motion, mean vertical motion and required subsidence in the $2-4^{\circ}$ outer convective area based on a moist static energy budget analysis. Other results suggest that parameterization schemes should include the effects of Cb overshoot cooling and extra-cloud subsidence at values of h higher than the observed \bar{h} . Deep convection seems well related to low level (sfc to 800 mb) convergence as noted by Cho and Ogura (1974), while shallow clouds are probably more closely related to low level winds, turbulence and humidities. The effects of ice phase transitions are probably negligible except in areas of extremely intense Cb convection. Spectral cloud parameterization schemes may have to adjust the types of clouds used according to the type of organization of the deep convection. Vertical momentum fluxes by clouds should be parameterized as discussed below.

Sea Surface Fluxes. Warm tropical ocean waters are important energy sources for tropical cyclones, Palmén, 1948; 1957; Gray, 1975a. The storms characteristically weaken as they move over colder waters (Brand, 1971).

The sea surface to air fluxes of moist static energy (h) found in the recent study of Frank (1976) are smaller than those reported in most previous empirical studies (Table 7). The results of the current study should be the best estimate due to the very large size of the data set used.

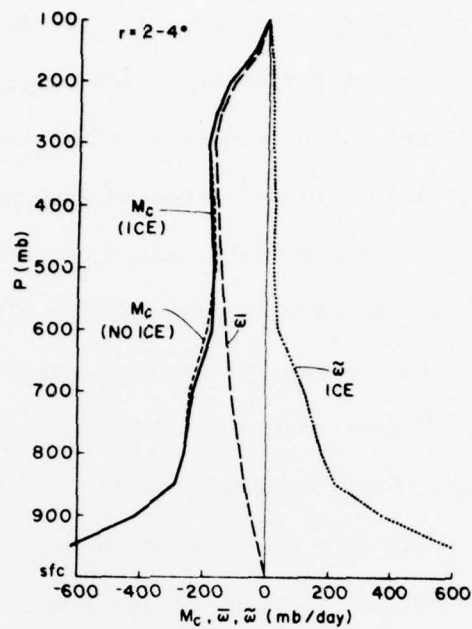


Fig. 27. Cloud mass flux profiles ($2-4^\circ$), mean vertical motion (ω) and extra-cloud subsidence ($\tilde{\omega}$). The effect of including ice phase transitions is shown.

TABLE 7

Sea Surface to Air Fluxes of Moist Static Energy (h) ($\text{cal/cm}^2 \text{ day}$)

<u>Study</u>	<u>h Fluxes</u>	<u>Region</u>
Present Study	1470 820	(0-80 km) (80-220 km)
<hr/>		
Daisy (Riehl & Malkus)		
August 25	1019	(0-130 km)
August 27	1675	(0-130 km)
Hilda (Hawkins & Rubsam)	~ 2560	(16-130 km)
Hilda (Leipper)	~ 4150	(~ 0 -240 km)
Inez (Hawkins & Imbembo)	~ 4018	(18-90 km)
(Malkus & Riehl)	3140	(30-90 km)

A constant sensible heat/evaporation coefficient of 1.5×10^{-3} applied to the 900 mb winds seems adequate to compute fluxes of these quantities from classical bulk aerodynamic formulas. A variable drag coefficient seems to yield better estimates of momentum and kinetic energy fluxes at the sea surface.

Radiation. Diurnal variations in tropical storm convection and temperatures are observed indicating that cloud/cloud free radiation differences should be incorporated into tropical cyclone models. Precipitation is maximum in the late morning and minimum in the evening, but the variation is only about 15%. Middle-level temperatures are warmest during the day. The radiational forcing occurs day and night and may well be a factor in such important storm features as the middle level inflow. Since the dominant factor in the radiation budget is the existence of dense cirrus cover, the extent of the cirrus shield must be predicted. The importance of radiational forcing is also stressed in observational studies by Jacobson and Gray (1976) and Foltz (1976).

Angular Momentum. In addition to the importance of horizontal eddy transports of momentum mentioned above, it must be noted that the Coriolis torque term (fV_r) does not integrate to zero in a region containing persistent northerly or southerly flow. At large radii this may become a major term in the angular momentum budget.

Vertical eddy fluxes of momentum by cumulus clouds are required to explain the observed circulation. They should be included in cumulus parameterization schemes wherever vertical wind shears are significant. As a first approximation, angular momentum can be treated as a conserved quantity in clouds.

Kinetic Energy. The use of mean circulation quantities alone gives a poor facsimile of the true kinetic energy budget. The sea surface

dissipation, mean circulation transport, and mean circulation generation terms tend to balance. This has often led to the neglect of eddy processes. However, eddy fluxes are large, and internal dissipation and eddy generation are substantial - perhaps dominant. The large scale storm circulation is a strong source of kinetic energy exporting about 4.8 watts/m^2 averaged over the $0-10^\circ$ radius region. This indicates that tropical cyclones may play a significant role in the tropical general circulation during certain seasons.

Water Budget. Due to the basic pattern of lower and middle tropospheric inflow and upper tropospheric outflow, tropical cyclones converge large quantities of water vapor. This phenomenon is enhanced by above average surface evaporation of sea water due to high surface winds. A small part of this water vapor convergence goes into increased humidity levels in the inner storm, but most falls out as precipitation.

The vertically integrated water budget of the composite steady state typhoon is shown in Fig. 28. Horizontal convergence of q was observed, and precipitation was estimated from rainfall studies by Miller (1958) and Gray et al. (1975). Evaporation was computed as a residual. The results seem realistic except for an apparent overestimate of evaporation from $4-6^\circ$ and an underestimate from $6-8^\circ$ - probably the result of a slight error in the $r = 6^\circ$ radial wind profile.

It is interesting to note that while about 75% of the observed $0-2^\circ$ precipitation results from horizontal convergence of water vapor, nearly 65% of the $0-6^\circ$ precipitation may be attributed to evaporation within that area. The $0-6^\circ$ evaporation is about double mean tropical values, primarily due to high winds. Hence, nearly 1/3 of the $0-6^\circ$ precipitation results from this anomalous evaporation. Tropical cyclones extract large mounts of extra energy from the sea.

WATER BUDGET (cm/day)						
CONVERGENCE OF q	6.7	1.2	-0.7	0.1	-0.1	-0.1
PRECIPITATION	9.0	2.3	0.7	0.7	0.7	0.7
REQUIRED EVAPORATION	↑ 2.3	↑ 1.1	↑ 1.4	↑ 0.6	↑ 0.8	↑ 0.8
	0°	2°	4°	6°	8°	10° 12°

Fig. 28. Water budget for 0-12° region. Evaporation values shown are the amounts required to achieve balance.

Typhoon Rainfall. N.W. Pacific rainfall data from small island stations were analyzed to determine the mean rainfall rates by quadrant for the 0-4° radius area (Fig. 29). No corrections were made for orographic effects or measurement errors. The values shown are for the 0-2° band and the 2-4° band for the four quadrants (the grid is aligned with the direction of storm motion toward the top of the page). Also shown are the radial band averages for all four quadrants. No striking asymmetries are observed, but rainfall does seem to be highest in the right rear quadrant. This finding contradicts earlier estimates of strong rainfall maxima in the right front quadrant (Cline, 1962; Schoner, 1957). Since most previous tropical cyclone rainfall studies have been performed for storms at or near continental landfall, it is possible that the previously observed right front quadrant maxima are orographic in origin due to onshore flow. Under such conditions suppressed convection would be expected in the front left quadrant where off-shore flow prevails.

COMBINED HOURLY & JAPANESE DATA

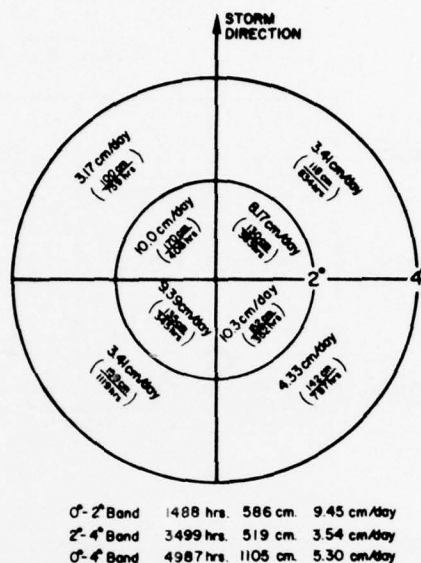


Fig. 29. Mean precipitation around tropical cyclone based on hourly data from 9 island stations and 12 hourly-data from 4 Japanese island stations.

Dunn and Miller (1964), have proposed that the precipitation pattern of low latitude storms is symmetrical with a right front quadrant maximum developing as the storms move poleward.

The hourly rainfall data were also used to determine the frequency and intensity of rainfall occurrences during typhoon passage near an island station. Table 8 shows the percentages of the total time in which various rainfall rates were recorded for each radial band.

It is interesting to note the relatively small percentage of the time that moderate to heavy rains ($\geq .1$ in/hour) fell. Such rainfall rates were recorded only 35% of the time in the highly active 0-2° region and but 17% of the time in the 2-4° band. Outside the 4° radius rainfalls of this intensity were not often recorded (3-6% of the time). Substantial amounts of light rain (.01-.10 in/hour) were recorded inside

TABLE 8

Rainfall Rates

Rainfall Rate in/hour	Percent of Total Storm Passage Time						
	<u>0-2⁰</u>	<u>2-4⁰</u>	<u>4-6⁰</u>	<u>6-8⁰</u>	<u>8-10⁰</u>	<u>10-12⁰</u>	<u>12-14⁰</u>
0-trace	30	59	80	87	89	89	90
.01-.1	35	24	14	10	7	7	7
.1-.3	19	11	4	2	3	2	2
.3-.9	13	5	2	1	1	2	1
>.9	3	1	<1	<1	<1	<1	<1

6⁰. It is possible that some of this rain was due to orographic effects resulting from elevated terrain, strong winds, and very high humidities. The above average rainfall recorded in the 4-6⁰ band seems to result primarily from an above normal incidence of light rainfall and slightly above average moderate rainfall (.1-.3 in/hour). Since this area is observed to be relatively cloud free, except for occasional outer rainbands, at least part of the observed positive anomaly in precipitation may have been orographic in origin.

The results of this rainfall study indicate that typhoon precipitation is primarily concentrated in localized heavy convective regions. The incidence of 2-4⁰ band rainfall is only slightly greater than was found for N.W. Pacific cloud clusters by Ruprecht and Gray (1976). The inner core (0-2⁰) area shows a much larger incidence of rainy episodes than is found in cloud clusters as expected. The frequencies of moderate to heavy rainfall (>.1 in/hr) agree relatively well with the convective

cloud covers inside 200 miles of ~5% Cb and ~25% total cumulus cloud cover reported by Malkus et al. (1961) and Gentry (1964).

8. SUMMARY

A number of new findings regarding the structure, dynamics and behavior of tropical cyclones have been summarized. However, much additional observational and modeling work remains. An enormous data set using many types of observations from various regions has been assembled at CSU. More data is continually being acquired. This is the largest tropical cyclone data sample assembled. The results of this paper are in many ways only preliminary findings. The researchers are confident that current and future research efforts will significantly improve tropical cyclone forecasting skills and improve our overall understanding of tropical weather systems.

ACKNOWLEDGEMENTS

The authors wish to express their gratitude to Mr. Dennis Shea, Dr. Eberhard Ruprecht, Mr. Raymond Zehr, Mr. William Fingerhut, Major Charles Arnold and Captain Steven Erickson for information concerning their research findings. Mr. Edwin Buzzell has been responsible for most of the numerical data processing. Thanks are also extended to Mrs. Barbara Brumit and Mrs. Dianne Schmitz for their assistance in manuscript preparation.

BIBLIOGRAPHY

- Anthes, R., S. L. Rosenthal and J. W. Trout, 1971: Preliminary results from an asymmetric model of the tropical cyclone. Mon. Wea. Rev. 99, 744-758.
- Arnold, C. A., 1977: Forthcoming CSU report on tropical cyclone convection using DMSP satellite data.
- Brand, S., 1971: The effects on a tropical cyclone of cooler surface waters due to upwelling and mixing produced by a prior tropical cyclone. J. Appl. Meteor. 10, 865-874.
- Carrier, G. F., A. L. Hammond and O. D. George, 1971: A model of the mature hurricane. J. Fluid Mech. Vol. 47, Part 1, 145-170 pp.
- Cho, H. R. and Y. Ogura, 1974: A relationship between cloud activity and the low-level convergence as observed in Reed-Recker's composite easterly waves. J. Atmos. Sci., 31, 2058-2065.
- Cline, I. M., 1962: "Tropical Cyclones", the Macmillan Co., New York, 301 pp.
- Dunn, G. E. and B. I. Miller, 1964: "Atlantic Hurricanes", 2nd ed., Louisiana St. U. Press, Baton Rouge, 377 pp.
- Dvorak, V. F., 1975: Tropical cyclone intensity analysis and forecasting from satellite imagery. Mon. Wea. Rev., 103, 5, 420-430.
- Erickson, S., 1977: Forthcoming CSU report on tropical cyclone genesis using DMSP satellite data.
- Fett, N. W. 1966: Upper level structure of the formative tropical cyclone, Mon. Wea. Rev., 99, 1, 9-18.
- Foltz, Gary S., 1976: Diurnal variation of the tropospheric energy balance. M.S. Thesis. Colo. State Univ., Atmos. Sci. Paper No. 262, Ft. Collins, CO, 135 pp.
- Frank, W. M., 1976: The structure and energetics of tropical cyclones. Colo. State Univ., Atmos. Sci. Paper No. 258, Ft. Collins, CO, 180pp.
- George, J. E., 1975: Tropical cyclone motion and surrounding parameter relationships. Colo. State Univ., Atmos. Sci. Paper No. 214, 105 pp.
- Gentry, R. C., 1964: A study of hurricane rainbands. National Hurricane Res. Proj. Rept. No. 69, 85 pp., (available from NOAA Weather Bureau, Miami office).
- Gray, W. M., 1962: On the balance of forces and radial accelerations in hurricanes. Quart. J. Roy. Meteor. Soc., 88, 430-458 pp.

BIBLIOGRAPHY (cont'd)

- Gray, W. M., 1967: The mutual variation of wind, shear and baroclinicity in the cumulus convective atmosphere of the hurricane. Mon. Wea. Rev., 95, 55-73.
- Gray, W. M. 1968: Global view of the origin of tropical disturbances and storms. Mon. Wea. Rev., 96, 669-700.
- Gray, W. M., 1973: Cumulus convection and large scale circulations, Part I: Broadscale and meso-scale interactions, Mon. Wea. Rev., 101, 839-855 pp.
- Gray, W. M., 1975a: Tropical cyclone genesis. Colo. State Univ., Atmos. Sci. Paper No. 234; Ft. Collins, CO, 119 pp.
- Gray, W. M. 1975b: Tropical cyclone genesis in the western North Pacific. ENVPREDRSCHFAC Technical Paper No. 16-75, Monterey, CA, 66 pp.
- Gray, W. M. and D. J. Shea, 1973: The hurricane's inner core region, II. Thermal stability and dynamic characteristics, J. Atmos. Sci., 30, 1565-1576.
- Gray, W. M. and D. J. Shea, 1976: Data summary of NOAA's hurricane inner-core radial leg flight penetrations 1957-1967, 1969. Colo. State Univ., Atmos. Sci. Paper No. 257, Ft. Collins, CO, 245 pp.
- Gray, W. M., E. Ruprecht, and R. Phelps, 1975: Relative humidity in tropical weather systems, Mon. Wea. Rev., 103, 8, 685-690.
- Jordan, C. L., 1958: Mean soundings for the West Indies area. J. Appl. Meteor., 15, 91-97.
- Hawkins, H. F., and D. T. Rubsam, 1968: Hurricane Hilda, 1964: II. Structure and budgets of the hurricane on October 1, 1964. Mon. Wea. Rev., 99, 427-434.
- Hawkins, H. F. and S. M. Imbembo, 1976: The structure of a small, intense hurricane - Inez 1966. Mon. Wea. Rev. 104, 418-442 pp.
- Jacobson, R. W., Jr. and W. M. Gray, 1976: Diurnal variation of oceanic deep cumulus convection. Colo. State Univ., Dept. of Atmos. Sci. Paper No. 243, Ft. Collins, CO, 106 pp.
- Kasahara, A., 1961: A numerical experiment on the development of a tropical cyclone. J. Meteor. 18, No. 3, 259-282.
- Kurihara, Y. and R. E. Tuleya, 1974: Structure of a cyclone developed in a three-dimensional numerical simulation model. J. Atmos. Sci. 31, No. 4, 893-919 pp.
- LaSeur, N. E. and H. F. Hawkins, 1963: An analysis of hurricane Cleo, (1958) based on data from research reconnaissance aircraft. Mon. Wea. Rev. 91, 694-709 pp.

BIBLIOGRAPHY (cont'd)

- Leipper, D. F., 1967: Observed ocean conditions and Hurricane Hilda, 1964. J. Atmos. Sci., 24, 182-196.
- Lopez, R. E., 1973: Cumulus convection and larger scale circulations. Part II: Cumulus and mesoscale interactions. Mon. Wea. Rev., 101, 856-870 pp.
- Malkus, J. S., C. Ronne and M. Chaffee, 1961: Cloud patterns in Hurricane Daisy, 1958. Tellus, 13, 8-30.
- Mathur, M. B., 1975: Development of a banded structure in a numerically simulated hurricane. J. Atmos. Sci. 32, 3, 512-522 pp.
- Miller, B. I., 1958: Rainfall rates in Florida hurricanes. Mon. Wea. Rev., 86(7), 258-264.
- Miller, B. I., 1962: On the momentum and energy balance of hurricane Helene (1958). National Hurricane Res. Proj. Rept. No. 53, 19 pp. (Available from NOAA Weather Bureau, Miami office).
- Ogura, Y., 1964: Frictionally controlled, thermally driven circulations in a circular vortex with application to tropical cyclones. J. Atmos. Sci. 21, 610-621 pp.
- Ooyama, K., 1969: Numerical simulation of the life cycle of tropical cyclones. J. Atmos. Sci., 26, 3-40.
- Palmén, E. H., 1948: On the formation and structure of tropical cyclones. Geophysica, Helsinki, 31, 26-38 pp.
- Palmén, E. H., 1957: A review of knowledge on the formation and development of tropical cyclones. Proc. Tropical Cyclone Symp., Brisbane, Dec. 1965, Wilke & Co., Ltd., Melbourne, 213-231.
- Ramage, C. S., 1973: Typhoon of October 1970 in the South China Sea: intensification, decay and ocean interaction. U.S. Environmental Prediction Research Facility, Navy Postgraduate School, Monterey, CA, ENVPREDSCHFAC Tech. Paper No. 4-73, 39 pp.
- Riehl, H., 1954: Tropical Meteorology. McGraw-Hill, New York, 392 pp.
- Riehl, H., 1972: Intensity of recurved typhoons. J. Appl. Meteor., 11, 613-615.
- Riehl, H. and J. S. Malkus, 1961: Some aspects of Hurricane Daisy, 1958. Tellus, 13, 181-213.
- Rosenthal, S. L., 1970: A circularly symmetric primitive equation model of tropical cyclone development containing an explicit water vapor cycle. Mon. Wea. Rev., 98, 643-663.

BIBLIOGRAPHY (cont'd)

- Ruprecht, E. and W. M. Gray, 1976: Analysis of satellite observed tropical cloud clusters. Part I: Structure and dynamics. Part II: Thermodynamics and diurnal variability. Tellus, 24, 391-425.
- Sadler, J. C., 1967: On the origin of tropical vortices. Working Panel on Trop. Dyn. Meteor. Naval Postgraduate School, Monterey, CA, 39-75.
- Schoner, R. W., 1957: Frequency and distribution of areal rainfall associated with tropical storms entering the coast of the United States (Texas to Maine). U.S. Weather Bureau, Hydrolic Svc. Div., Washington, DC, 60 pp. (unpublished).
- Shea, D. J., 1972: The structure and dynamics of the hurricane's inner core region. Colo. State Univ., Atmos. Sci. Paper No. 182, Ft. Collins, CO, 134 pp.
- Shea, D. J. and W. M. Gray, 1973: The hurricane's inner core region: I, Symmetric and asymmetric structure. J. Atmos. Sci., 30, 1544-1564.
- Sheets, R. C., 1967a: On the structure of Hurricane Janice (1958). National Hurricane Res. Lab. Rept. No. 76, 30 pp. (available from NOAA Weather Bureau, Miami office).
- Sheets, R. C., 1967B: On the structure of Hurricane Ella (1962). National Hurricane Res. Lab. Rept. No. 77, 33 pp. (available from NOAA Weather Bureau, Miami office).
- Sheets, R. C., 1968: On the structure of Hurricane Dora (1964). National Hurricane Res. Lab. Rept. No. 83, 64 pp. (available from NOAA Weather Bureau, Miami office).
- Sundquist, H., 1970: Numerical simulation of the development of tropical cyclones with a ten-level model, Part 1. Tellus 12, 359-390 pp.
- Tsui, K. S., G. J. Bell and P. C. W. Fung, 1977: Change in intensity of typhoons which develop cloud-plume outflow aloft. Quart. J. Roy. Meteor. Soc., 103, 151-156.
- Williams, K. T. and W. M. Gray, 1973: Statistical analysis of satellite observed cloud clusters in the western North Pacific. Tellus, 25, 178-201 pp.
- Yamasaki, M., 1968: Numerical simulation of tropical cyclone development with the use of primitive equations. J. Meteor. Soc. Japan 46, 178-201 pp.
- Zehr, R., 1976: Tropical disturbance intensification: Colo. State Univ., Atmos. Sci. Paper No. 259, Ft. Collins, CO (Being published).

